Supplementary information

Chalcogen and halogen surface termination coverage in MXenes – structure, stability, and properties

Martin Dahlqvist, Johanna Rosen
Materials Design, Department of Physics, Chemistry and Biology (IFM), Linköping University, SE-581 83 Linköping, Sweden
Corresponding authors: M. Dahlqvist (martin.dahlqvist@liu.se), J. Rosen (johanna.rosen@liu.se)

Table S1. PBE potential used for elements considered in this work.

Element	POTCAR	Valence electrons
Ti	Ti_pv	4s 3d 3p
Zr	Zr_sv	5s 4d 4p 4s
V	V_pv	4s 3d 3p
Nb	Nb_pv	5s 4d 4p
Ta	Ta_pv	6s 5d 5p
C	C	2p 2s
O	O	2p 2s
S	S	3p 3s
Se	Se	4p 4s
Te	Te	5p 5s
F	F	2p 2s
Cl	Cl	3p 3s
Br	Br	4p 4s
I	I	5p 5s

Ideal multilayer M_2CT_2

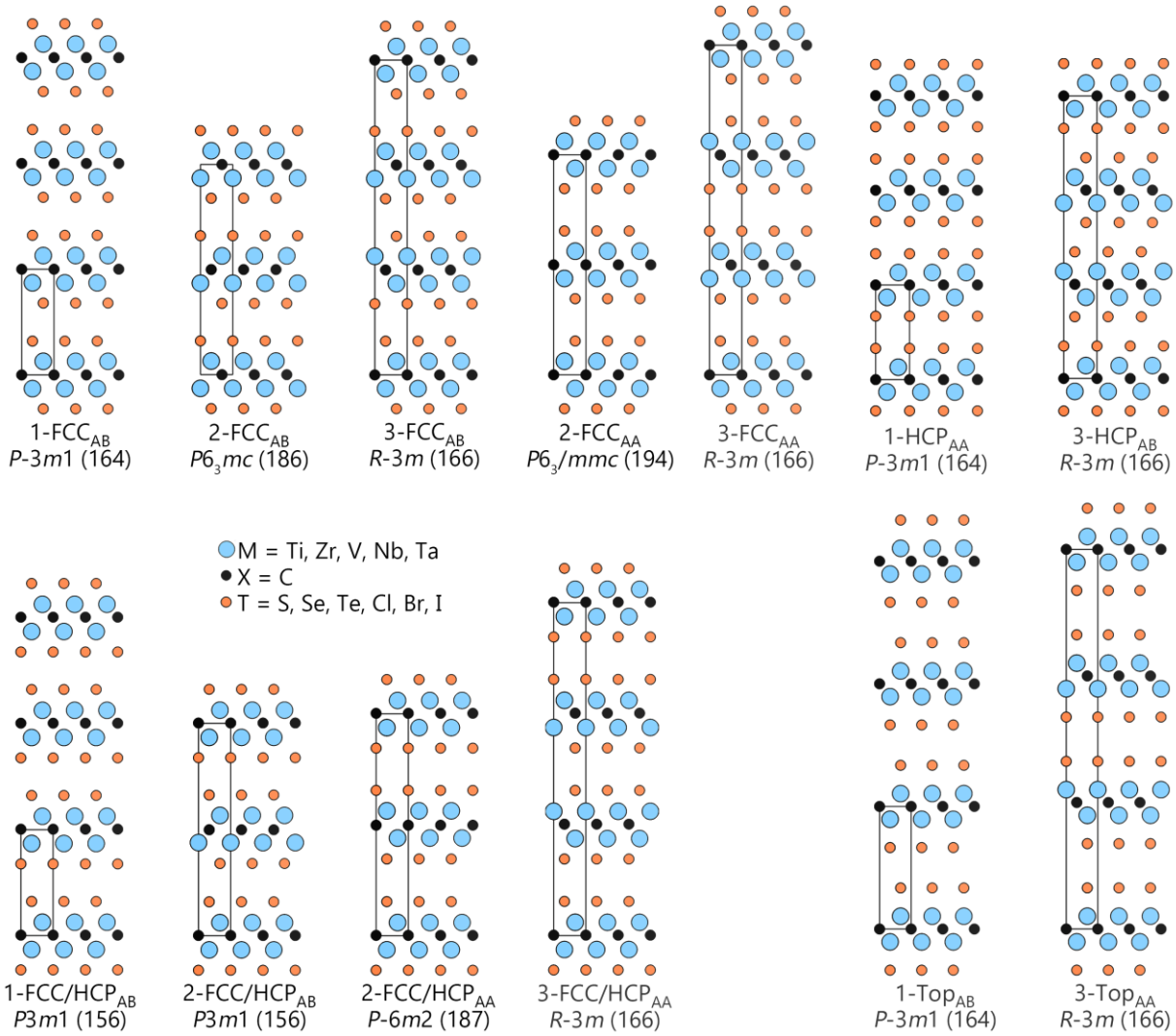

Figure S1. Schematic illustration of the different structures considered for multilayer M_2CT_2. Metal M in blue, carbon in black, and termination T in orange.

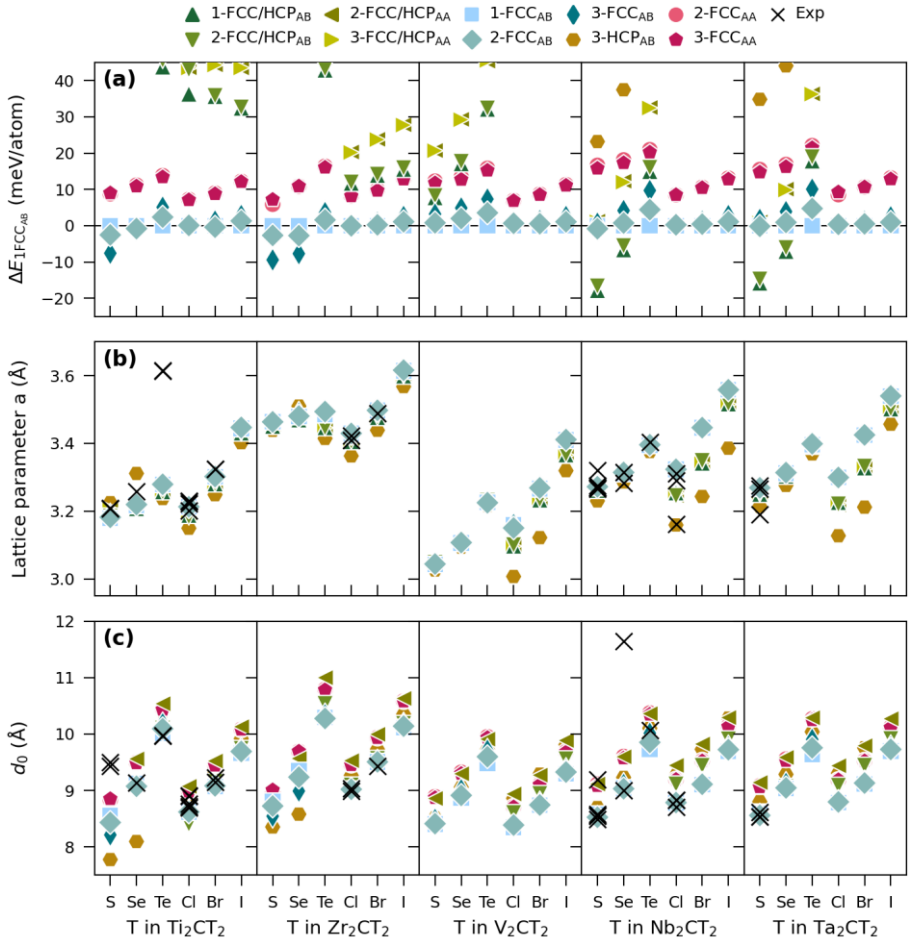

Figure S2. (a) Relative energies for various stackings compared to 1-FCC$_{AB}$. (b) In-plane lattice parameter *a* and (c) center-to-center spacing d_0 for various low-energy stackings considered for M_2CT_2. The exchange–correlation interactions were treated by van der Waals density functional (DFT-D3) developed by Grimme et al. [35].

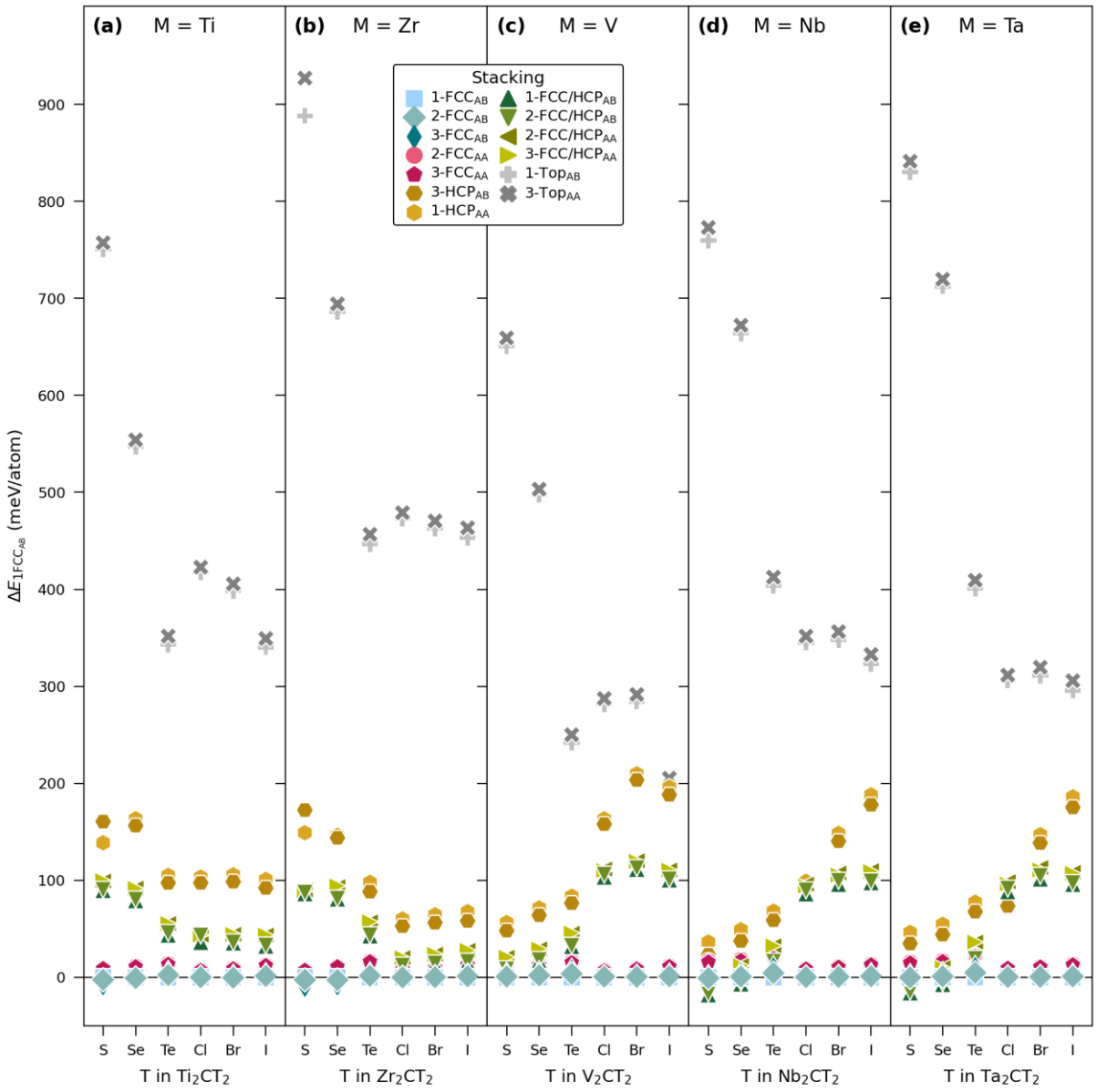

Figure S3. Relative energies for various stackings compared to 1-FCC$_{AB}$ using different termination T for (a) Ti_2CT_2, (b) Zr_2CT_2, (c) V_2CT_2, (d) Nb_2CT_2, and (e) Ta_2CT_2. The exchange–correlation interactions were treated by van der Waals density functional (DFT-D3) developed by Grimme et al. [35].

Table S2. Three stackings of lowest energy for M_2CT_2.

M_2CT_2	Stacking of lowest energy	Energy (eV/atom)	Stacking of 2nd lowest energy	Energy (eV/atom)	Stacking of 3rd lowest energy	Energy (eV/atom)
Ti_2CS_2	3-FCC_{AB}	-7.93003	2-FCC_{AB}	-7.92498	1-FCC_{AB}	-7.92244
Ti_2CSe_2	3-FCC_{AB}	-7.58131	2-FCC_{AB}	-7.58126	1-FCC_{AB}	-7.58046
Ti_2CTe_2	1-FCC_{AB}	-7.20157	2-FCC_{AB}	-7.19920	3-FCC_{AB}	-7.19648
Ti_2CCl_2	1-FCC_{AB}	-7.33472	2-FCC_{AB}	-7.33463	3-FCC_{AB}	-7.33419
Ti_2CBr_2	2-FCC_{AB}	-7.00184	1-FCC_{AB}	-7.00143	3-FCC_{AB}	-7.00017
Ti_2CI_2	1-FCC_{AB}	-6.55393	2-FCC_{AB}	-6.55261	3-FCC_{AB}	-6.55112
Zr_2CS_2	3-FCC_{AB}	-8.30066	2-FCC_{AB}	-8.29391	1-FCC_{AB}	-8.29123
Zr_2CSe_2	3-FCC_{AB}	-7.95000	2-FCC_{AB}	-7.94503	1-FCC_{AB}	-7.94229
Zr_2CTe_2	1-FCC_{AB}	-7.57109	2-FCC_{AB}	-7.56950	3-FCC_{AB}	-7.56749
Zr_2CCl_2	2-FCC_{AB}	-7.69252	1-FCC_{AB}	-7.69248	3-FCC_{AB}	-7.69234
Zr_2CBr_2	1-FCC_{AB}	-7.40891	2-FCC_{AB}	-7.40868	3-FCC_{AB}	-7.40798
Zr_2CI_2	1-FCC_{AB}	-7.02935	2-FCC_{AB}	-7.02826	3-FCC_{AB}	-7.02681
V_2CS_2	1-FCC_{AB}	-8.10955	2-FCC_{AB}	-8.10876	3-FCC_{AB}	-8.10635
V_2CSe_2	1-FCC_{AB}	-7.78290	2-FCC_{AB}	-7.78092	3-FCC_{AB}	-7.77801
V_2CTe_2	1-FCC_{AB}	-7.42376	2-FCC_{AB}	-7.42022	3-FCC_{AB}	-7.41642
V_2CCl_2	1-FCC_{AB}	-7.32488	2-FCC_{AB}	-7.32422	3-FCC_{AB}	-7.32411
V_2CBr_2	1-FCC_{AB}	-7.01302	2-FCC_{AB}	-7.01246	3-FCC_{AB}	-7.01160
V_2CI_2	1-FCC_{AB}	-6.59198	2-FCC_{AB}	-6.59090	3-FCC_{AB}	-6.58944
Nb_2CS_2	1-FCC/HCP_{AB}	-8.68788	2-FCC/HCP_{AB}	-8.68678	2-FCC_{AB}	-8.67093
Nb_2CSe_2	1-FCC/HCP_{AB}	-8.36264	2-FCC/HCP_{AB}	-8.36167	1-FCC_{AB}	-8.35607
Nb_2CTe_2	1-FCC_{AB}	-7.98056	2-FCC_{AB}	-7.97614	3-FCC_{AB}	-7.97085
Nb_2CCl_2	1-FCC_{AB}	-7.82935	2-FCC_{AB}	-7.82910	3-FCC_{AB}	-7.82883
Nb_2CBr_2	1-FCC_{AB}	-7.56438	2-FCC_{AB}	-7.56394	3-FCC_{AB}	-7.56316
Nb_2CI_2	1-FCC_{AB}	-7.21831	2-FCC_{AB}	-7.21722	3-FCC_{AB}	-7.21551
Ta_2CS_2	1-FCC/HCP_{AB}	-9.45829	2-FCC/HCP_{AB}	-9.45732	2-FCC_{AB}	-9.44270
Ta_2CSe_2	1-FCC/HCP_{AB}	-9.08417	2-FCC/HCP_{AB}	-9.08328	1-FCC_{AB}	-9.07715
Ta_2CTe_2	1-FCC_{AB}	-8.67671	2-FCC_{AB}	-8.67198	3-FCC_{AB}	-8.66666
Ta_2CCl_2	1-FCC_{AB}	-8.47695	2-FCC_{AB}	-8.47657	3-FCC_{AB}	-8.47636
Ta_2CBr_2	1-FCC_{AB}	-8.20167	2-FCC_{AB}	-8.20116	3-FCC_{AB}	-8.20046
Ta_2CI_2	1-FCC_{AB}	-7.83423	2-FCC_{AB}	-7.83329	3-FCC_{AB}	-7.83178

Table S3. Structural information for different stackings considered for simulating multilayer MXenes with corresponding Wyckoff sites. Specific structural data are here represented by relaxed Ti_2CSe_2.

Stacking	Space group	*a* (Å)	*c* (Å)	Wyckoff sites
1-FCC_{AB}	*P*-3*m*1 (164)	3.21756	9.12427	Ti1 2d (0.33333, 0.66667, 0.12883) C1 1a (0.00000, 0.00000, 0.00000) Se1 2d (0.33333, 0.66667, 0.68024)
2-FCC_{AB}	*P*6$_3$*mc* (186)	3.21938	18.14840	Ti1 2a (0.00000, 0.00000, -0.06472) Ti2 2b (0.33333, 0.66667, 0.56483) C1 2b (0.33333, 0.66667, 0.00000) Se1 2a (0.00000, 0.00000, 0.16065) Se2 2b (0.33333, 0.66667, 0.33939)
3-FCC_{AB}	*R*-3*m* (166)	3.22150	27.12200	Ti1 6c (0.00000, 0.00000, 0.37667) C1 3a (0.00000, 0.00000, 0.00000) Se1 6c (0.00000, 0.00000, 0.22596)
2-FCC_{AA}	*P*6$_3$/*mmc* (194)	3.21763	18.98990	Ti1 4f (0.33333, 0.66667, -0.06186) C1 2a (0.00000, 0.00000, 0.00000) Se1 4f (0.33333, 0.66667, 0.15369)
3-FCC_{AA}	*R*-3*m* (166)	3.21769	28.45810	Ti1 6c (0.00000, 0.00000, 0.70795) C1 3a (0.00000, 0.00000, 0.00000) Se1 6c (0.00000, 0.00000, 0.56412)
1-HCP_{AA}	*P*-3*m*1 (164)	3.37981	8.13743	Ti1 2d (0.33333, 0.66667, 0.13115) C1 1a (0.00000, 0.00000, 0.00000) Se1 2c (0.00000, 0.00000, 0.32977)
3-HCP_{AB}	*R*-3*m* (166)	3.31117	24.28670	Ti1 6c (0.00000, 0.00000, 0.37906) C1 3a (0.00000, 0.00000, 0.00000) Se1 6c (0.00000, 0.00000, 0.88515)
1-FCC/HCP_{AB}	*P*3*m*1 (156)	3.20826	9.12361	Ti1 1b (0.33333, 0.66667, 0.12158) Ti2 1c (0.66667, 0.33333, 0.86461) C1 1a (0.00000, 0.00000, 0.00000) Se1 1a (0.00000, 0.00000, 0.67224) Se2 1c (0.66667, 0.33333, 0.31822)
2-FCC/HCP_{AB}	*P*3*m*1 (156)	3.20877	18.29250	Ti1 1c (0.66667, 0.33333, -0.06758) Ti2 1b (0.33333, 0.66667, 0.06052) Ti3 1a (0.00000, 0.00000, 0.43717) Ti4 1b (0.33333, 0.66667, 0.56531) C1 1a (0.00000, 0.00000, 0.00000) C2 1c (0.66667, 0.33333, 0.49764) Se1 1c (0.66667, 0.33333, 0.15860) Se2 1b (0.33333, 0.66667, 0.33896) Se3 1c (0.66667, 0.33333, 0.66128) Se4 1a (0.00000, 0.00000, 0.83650)
2-FCC/HCP_{AA}	*P*-6*m*2 (187)	3.20567	19.11720	Ti1 2i (0.66667, 0.33333, 0.18531) Ti2 2h (0.33333, 0.66667, 0.30781) C1 2g (0.00000, 0.00000, 0.25000) Se1 2i (0.66667, 0.33333, 0.40204) Se2 2g (0.00000, 0.00000, 0.90303)
3-FCC/HCP_{AA}	*R*-3*m* (166)	3.20514	28.66480	Ti1 3a (0.00000, 0.00000, 0.37193) Ti2 3a (0.00000, 0.00000, 0.62356) C1 3a (0.00000, 0.00000, 0.00000) Se1 3a (0.00000, 0.00000, 0.89543) Se2 3a (0.00000, 0.00000, 0.76810)
1-Top_{AB}	*P*-3*m*1 (164)	3.14205	10.57930	Ti1 2d (0.33333, 0.66667, 0.10453) C1 1a (0.00000, 0.00000, 0.00000) Se1 2d (0.33333, 0.66667, 0.33483)
3-Top_{AA}	*R*-3*m* (166)	3.14175	32.73070	Ti1 6c (0.00000, 0.00000, 0.36713) C1 3a (0.00000, 0.00000, 0.00000) Se1 6c (0.00000, 0.00000, 0.55840)

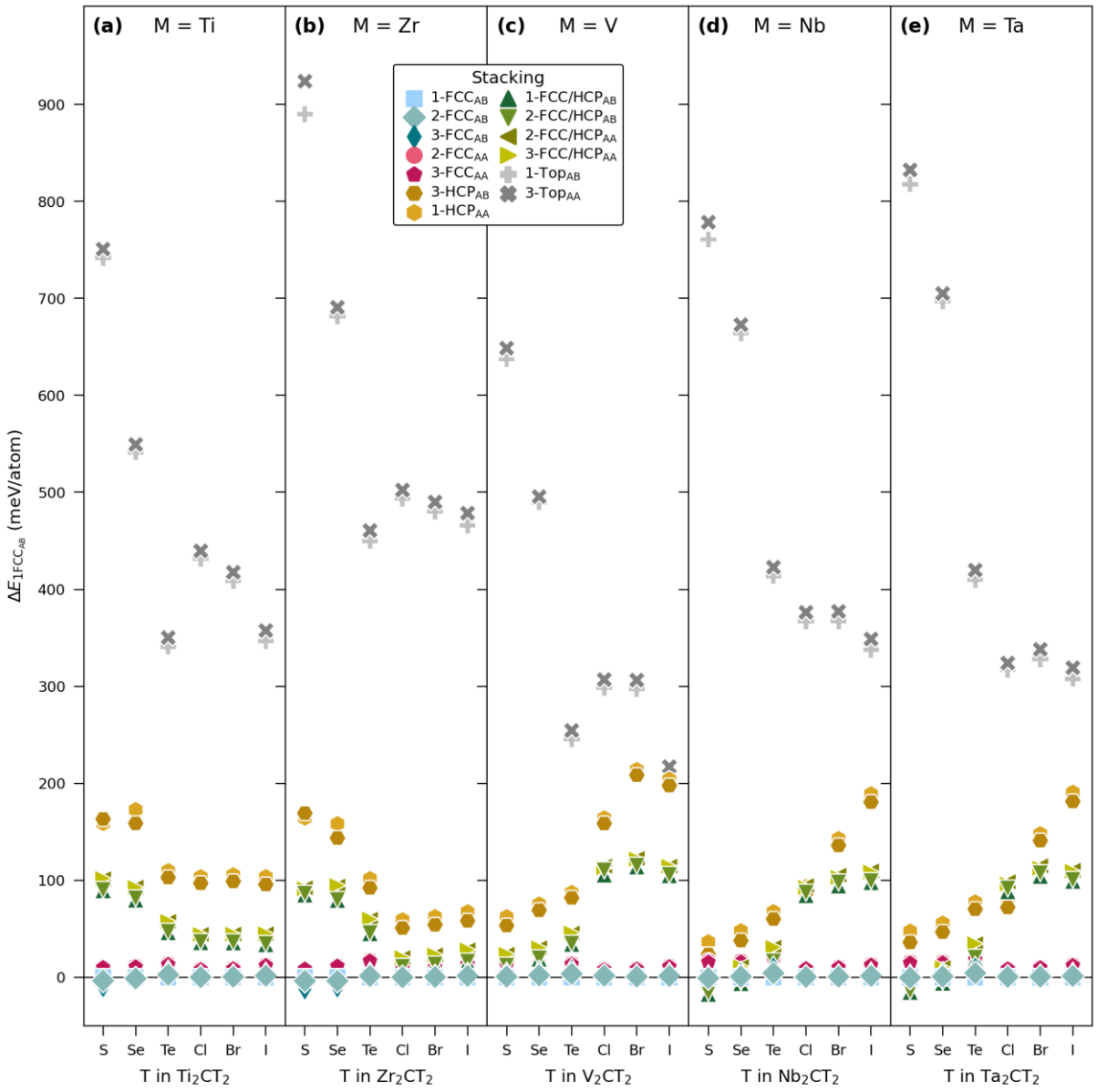

Figure S4. Relative energies for various stackings compared to 1-FCC$_{AB}$ using different termination T for (a) Ti_2CT_2, (b) Zr_2CT_2, (c) V_2CT_2, (d) Nb_2CT_2, and (e) Ta_2CT_2. The exchange–correlation interactions were treated by van der Waals density functional (rev-vdW-DF2) in the version developed by Hamada [36, 37].

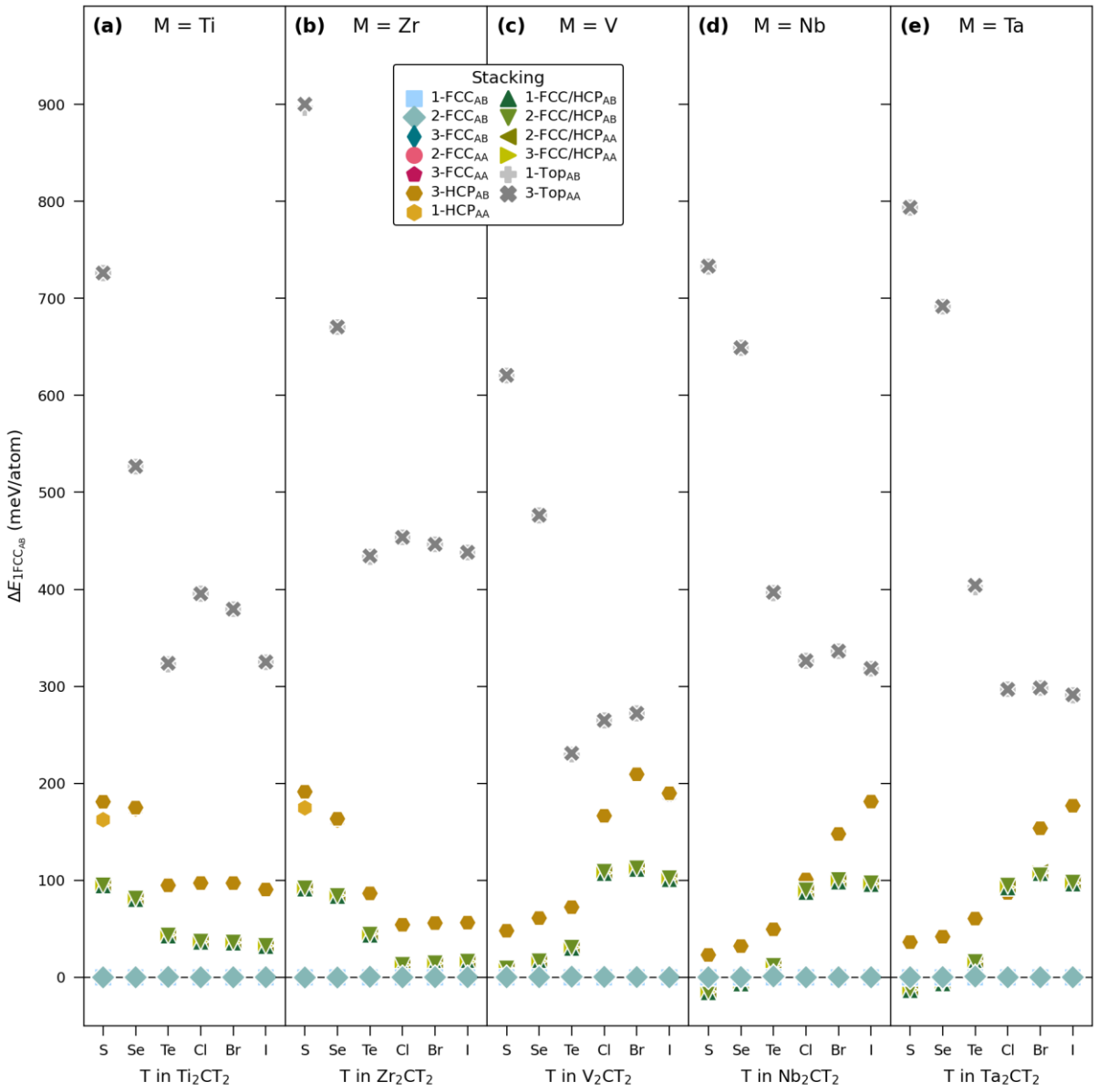

Figure S5. Relative energies for various stackings compared to 1-FCC$_{AB}$ using different termination T for (a) Ti_2CT_2, (b) Zr_2CT_2, (c) V_2CT_2, (d) Nb_2CT_2, and (e) Ta_2CT_2. No van der Waals interaction were considered.

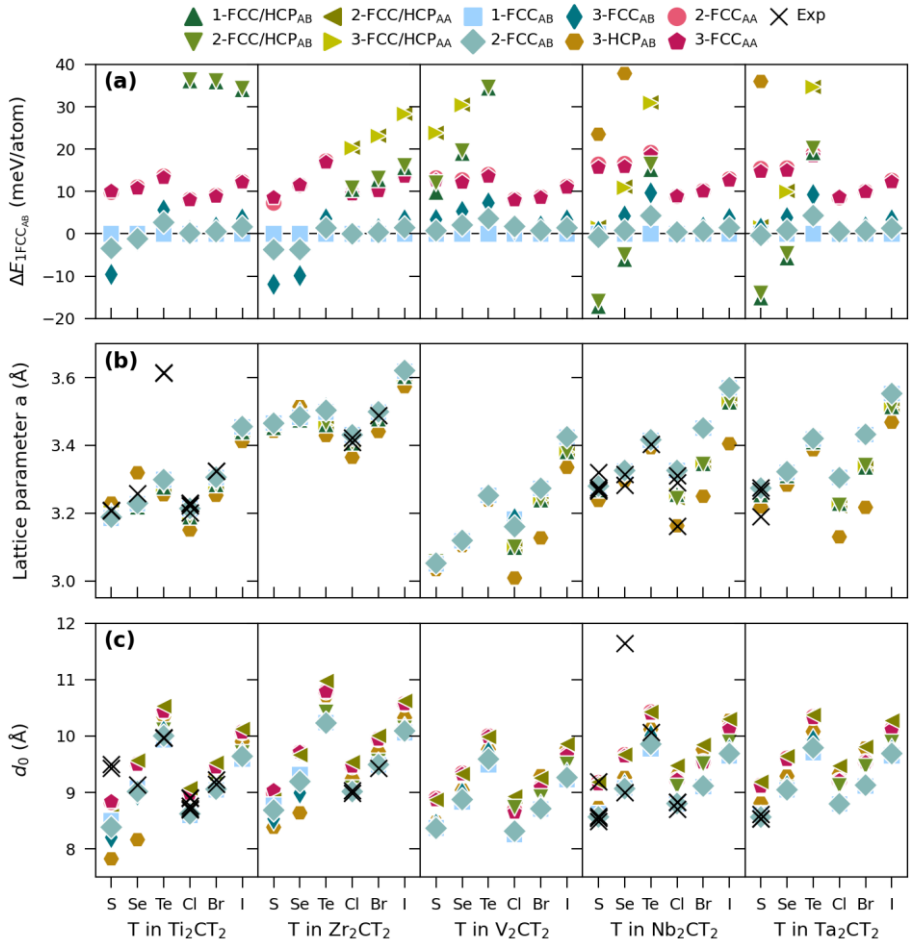

Figure S6. (a) Relative energies for various stackings compared to 1-FCC$_{AB}$. (b) In-plane lattice parameter *a* and (c) center-to-center spacing d_0 for various low-energy stackings considered for M_2CT_2. The exchange–correlation interactions were treated by van der Waals density functional (rev-vdW-DF2) in the version developed by Hamada [36, 37].

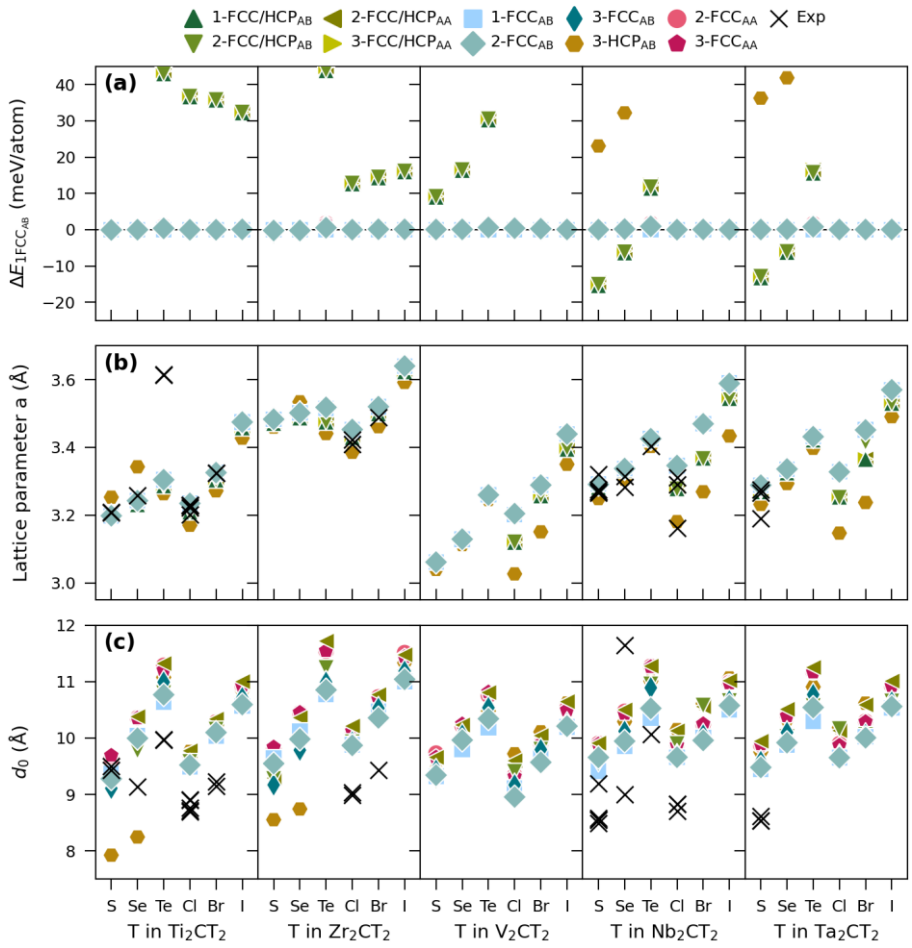

Figure S7. (a) Relative energies for various stackings compared to 1-FCC$_{AB}$. (b) In-plane lattice parameter *a* and (c) center-to-center spacing d_0 for various low-energy stackings considered for M_2CT_2. No van der Waals interaction were considered.

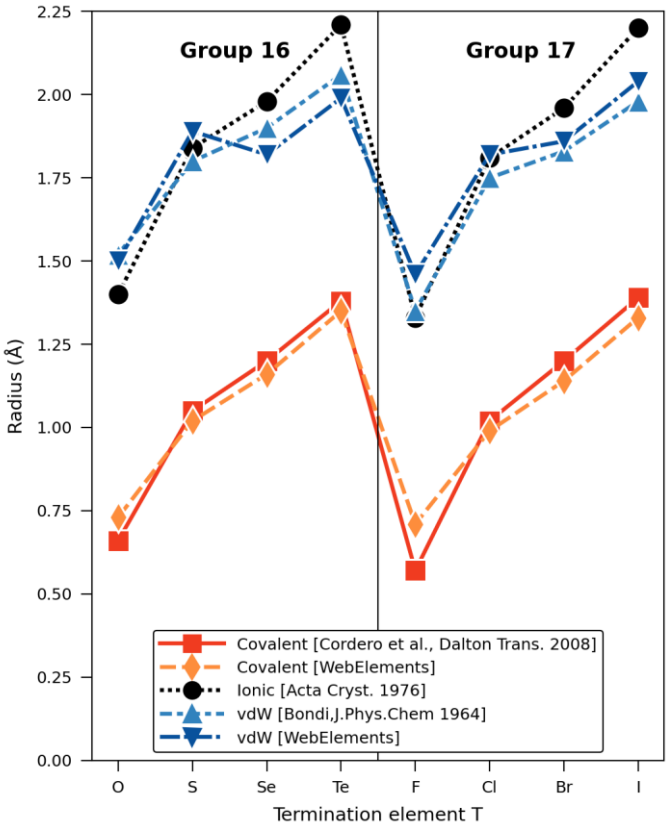

Figure S8. Covalent radius (red and orange)[48, 49], van der Waals radius (blue)[49, 50], and ionic raidus (black)[51] for different termination species from Group 16 and 17.

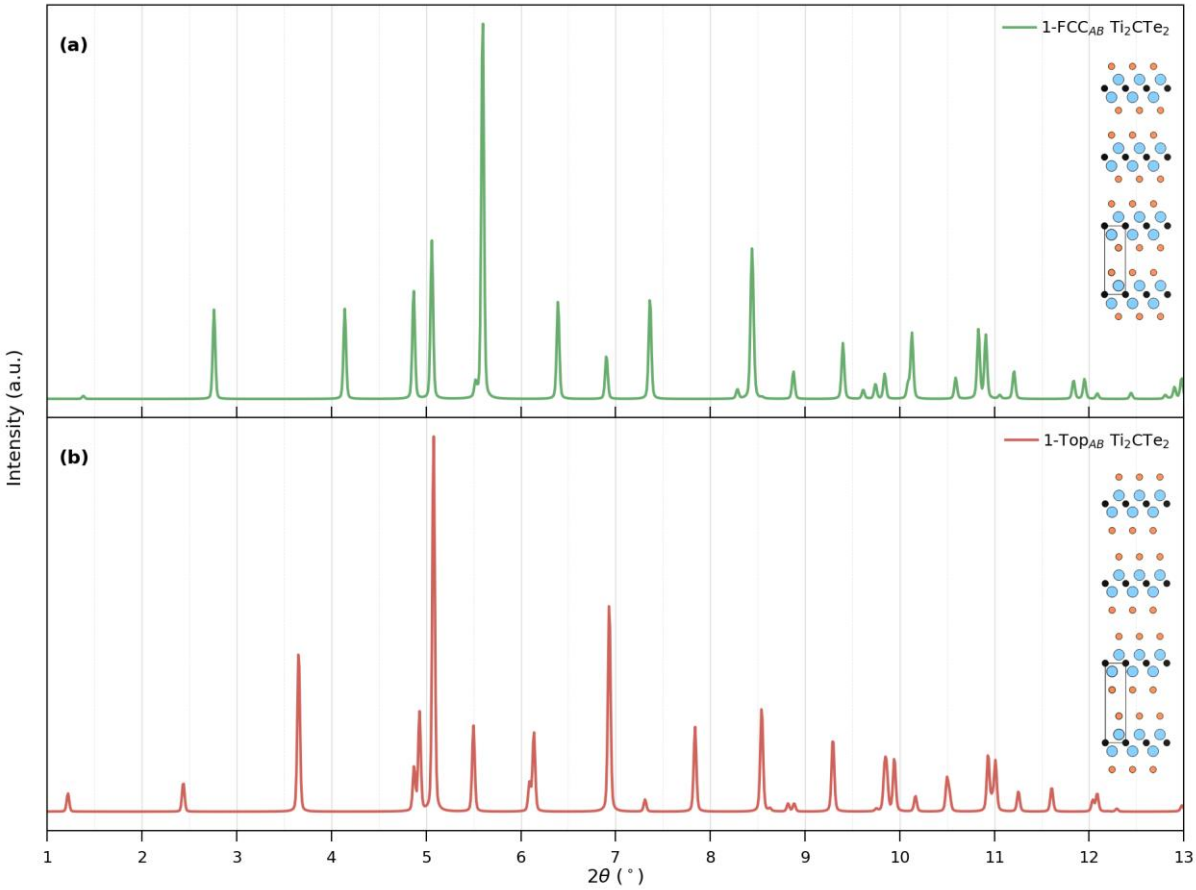

Figure S9. Simulated XRD for Ti_2CTe_2 with (a) 1-FCC_{AB} and (b) 1-Top_{AB} structure. Wavelength of 0.2412 Å have been used.

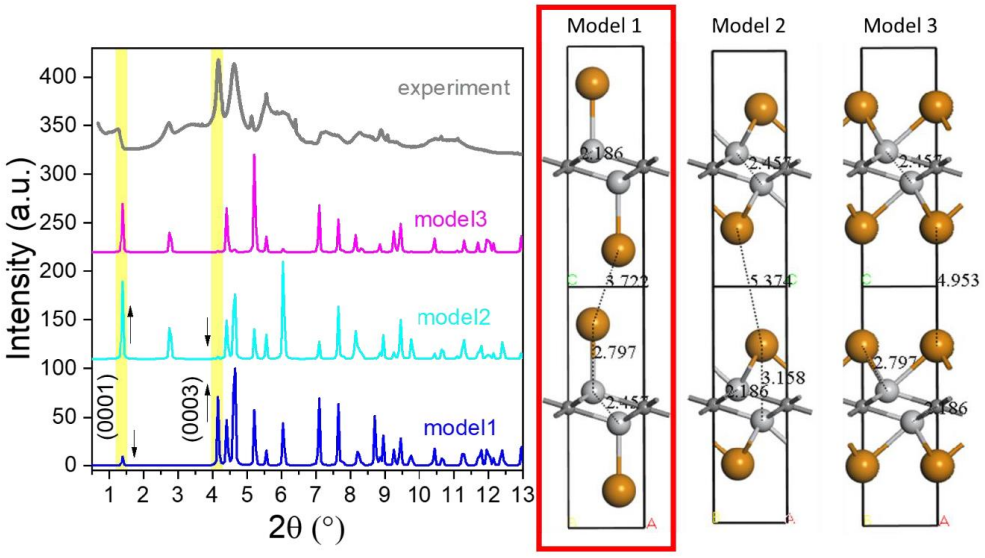

Figure S10. Comparison between simulated and experimental XRD patterns, measured with a wavelength of 0.2412 Å, for Ti_2CTe_x MXene. Figure retrived from Figure S38 in Ref. [10].

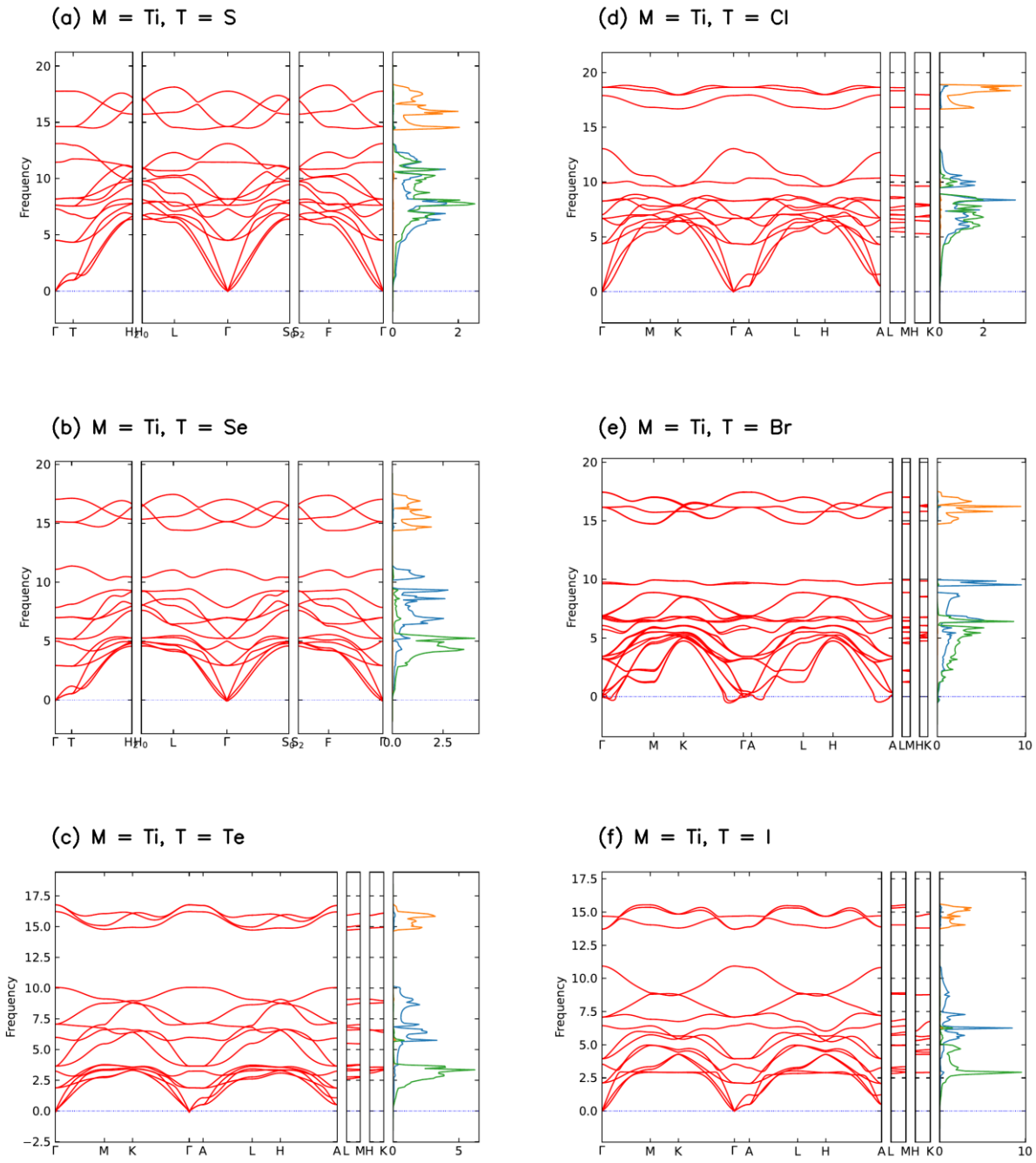

Figure S11. Phonon dispersion (left) and density of states (right) for lowest energy structures of Ti_2CT_2 for (a) T = S, (b) T = Se, (c) T = Te, (d) T = Cl, (e) T = Br, and (f) T = I.

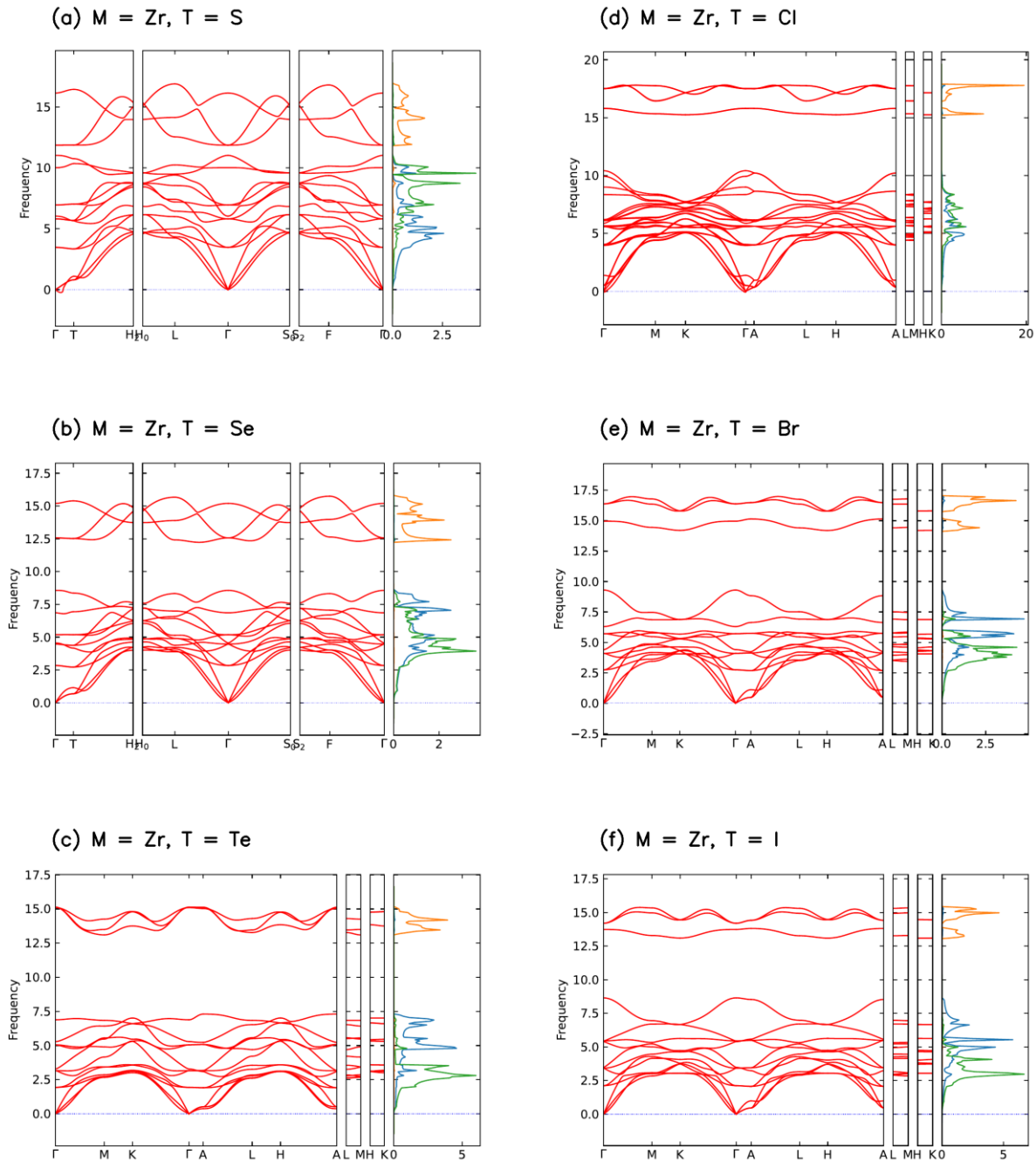

Figure S12. Phonon dispersion (left) and density of states (right) for lowest energy structures of Zr_2CT_2 for (a) T = S, (b) T = Se, (c) T = Te, (d) T = Cl, (e) T = Br, and (f) T = I.

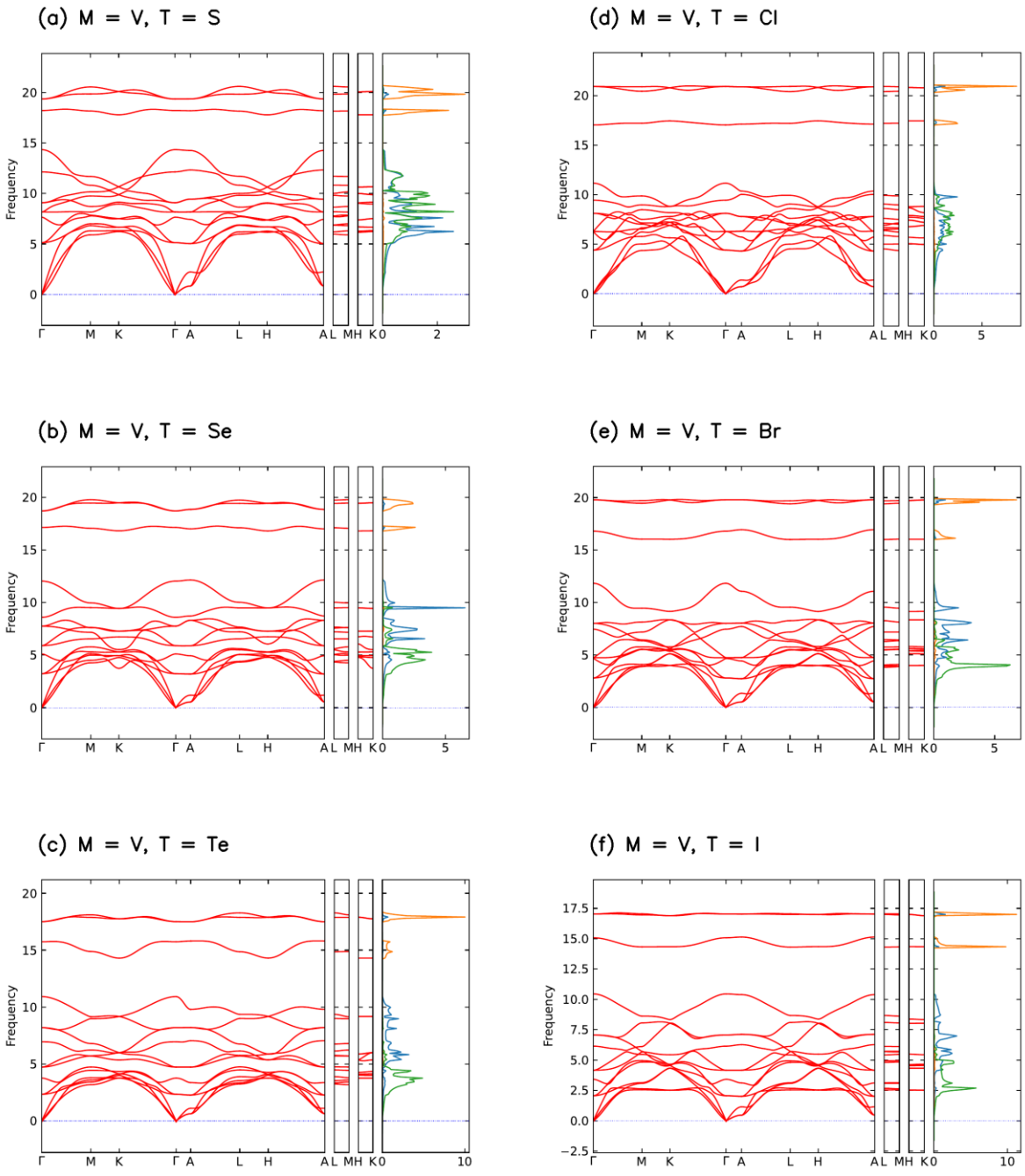

Figure S13. Phonon dispersion (left) and density of states (right) for lowest energy structures of V_2CT_2 for (a) T = S, (b) T = Se, (c) T = Te, (d) T = Cl, (e) T = Br, and (f) T = I.

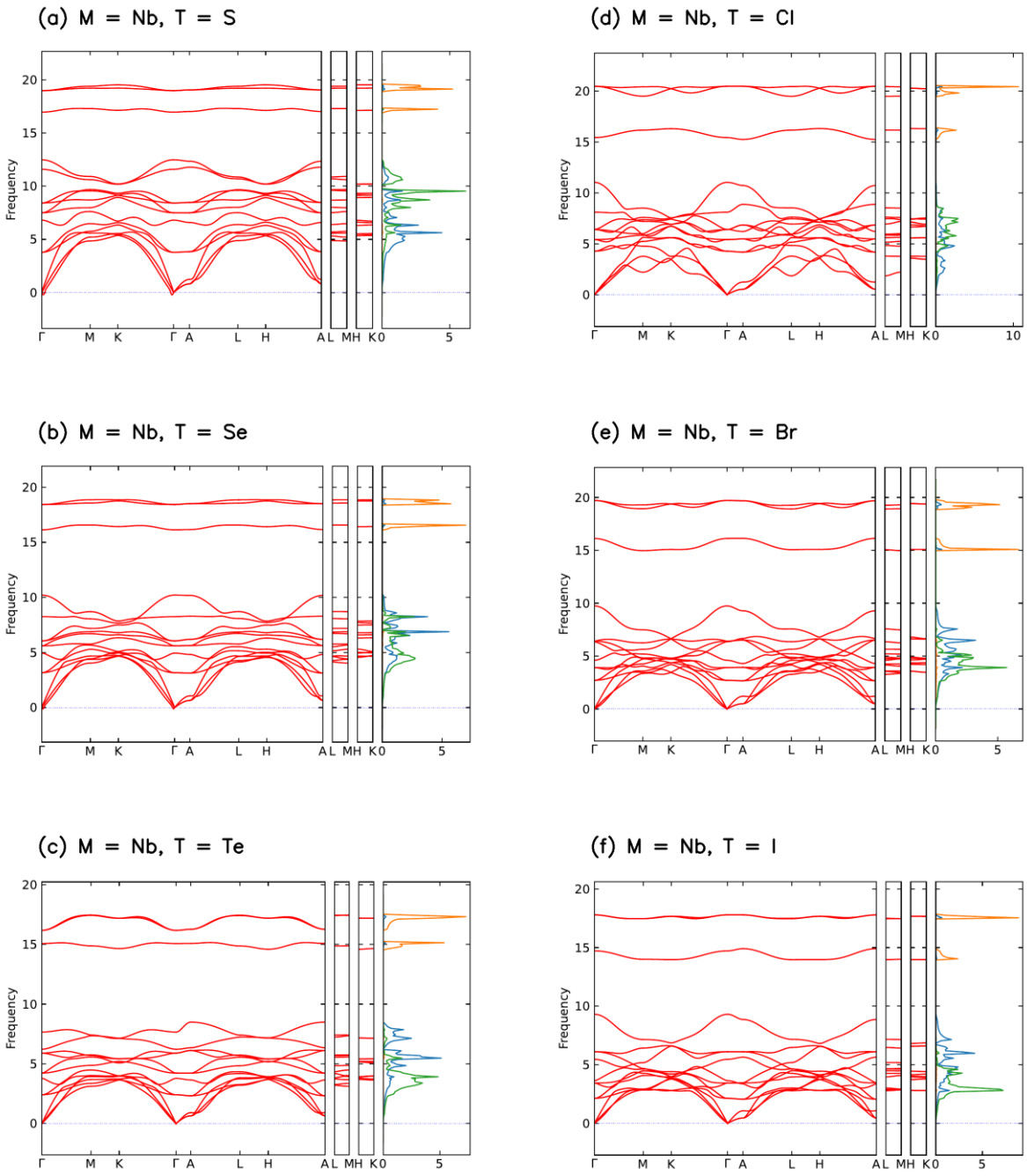

Figure S14. Phonon dispersion (left) and density of states (right) for lowest energy structures of Nb_2CT_2 for (a) T = S, (b) T = Se, (c) T = Te, (d) T = Cl, (e) T = Br, and (f) T = I.

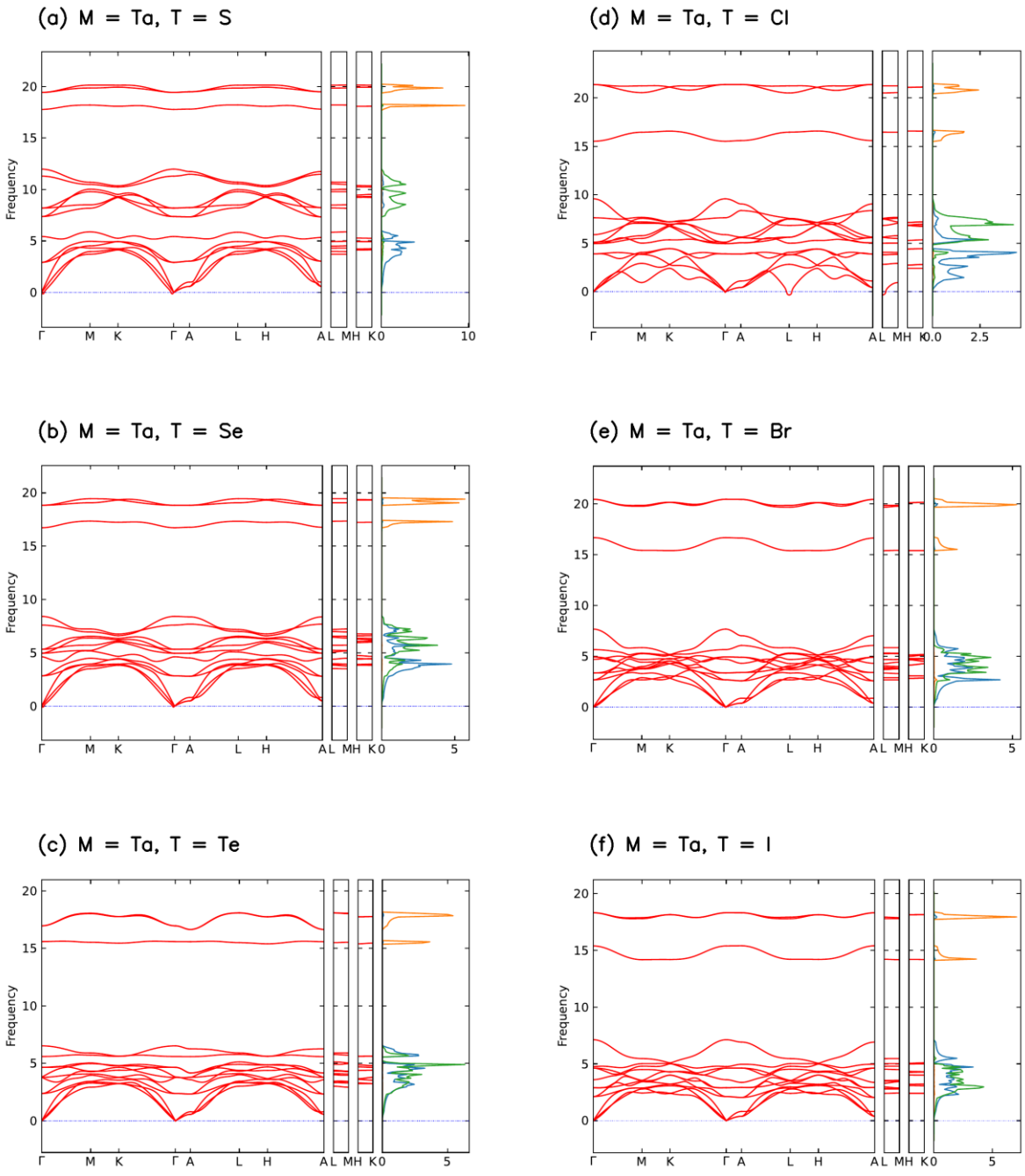

Figure S15. Phonon dispersion (left) and density of states (right) for lowest energy structures of Ta_2CT_2 for (a) T = S, (b) T = Se, (c) T = Te, (d) T = Cl, (e) T = Br, and (f) T = I.

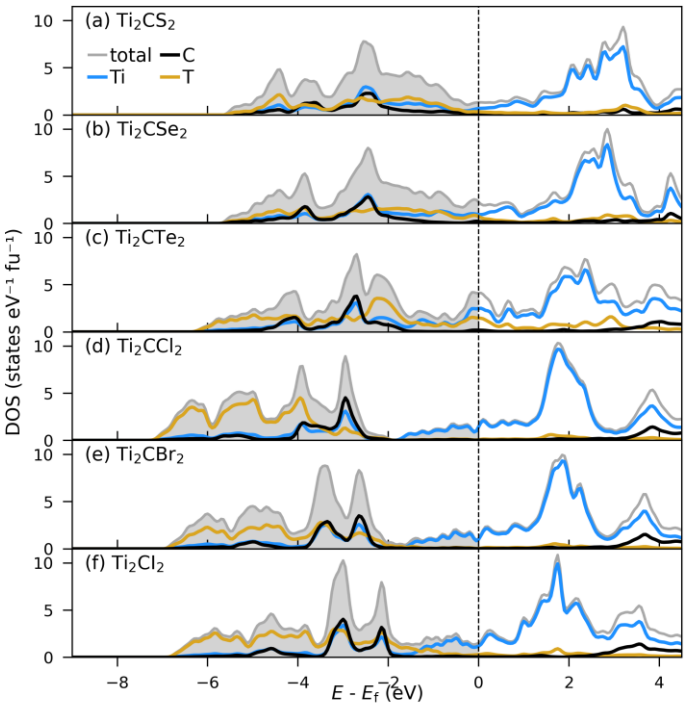

Figure S16. Electronic density of states for lowest energy structures of Ti_2CT_2 for (a) T = S, (b) T = Se, (c) T = Te, (d) T = Cl, (e) T = Br, and (f) T = I.

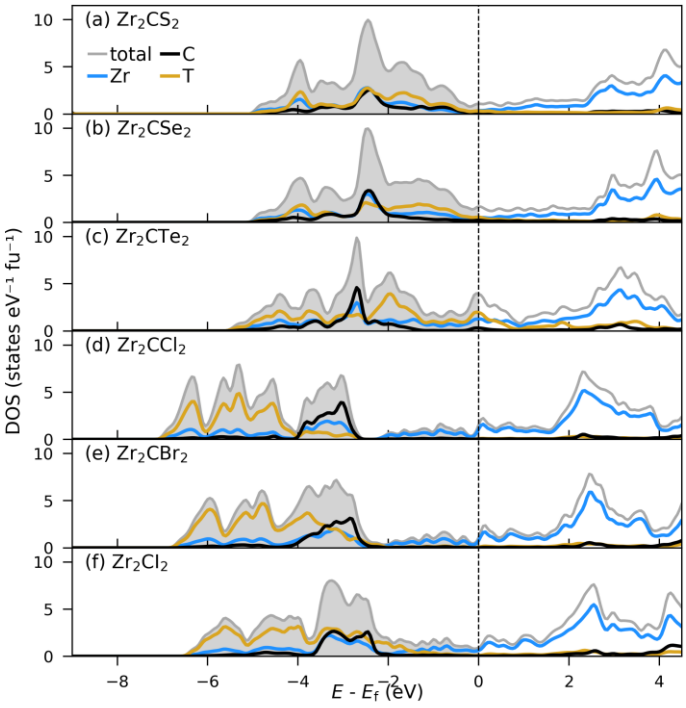

Figure S17. Electronic density of states for lowest energy structures of Zr_2CT_2 for (a) T = S, (b) T = Se, (c) T = Te, (d) T = Cl, (e) T = Br, and (f) T = I.

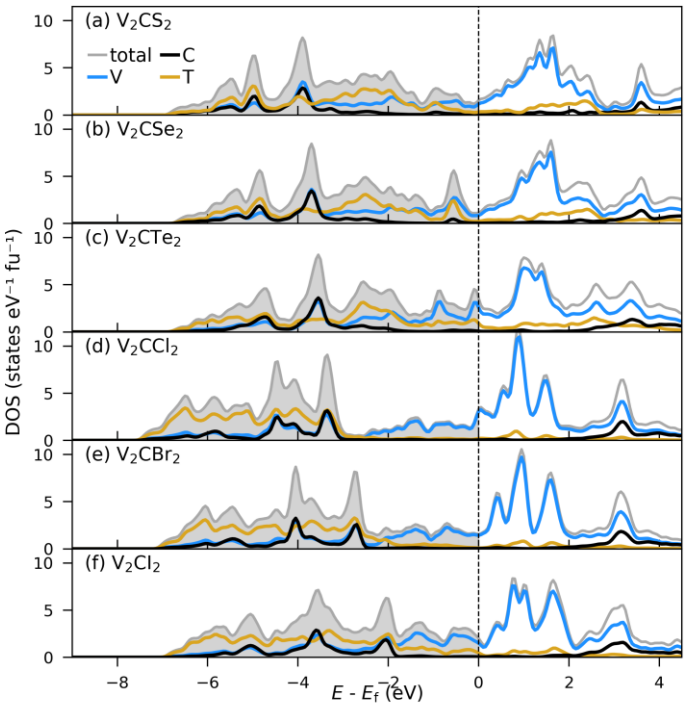

Figure S18. Electronic density of states for lowest energy structures of V_2CT_2 for (a) T = S, (b) T = Se, (c) T = Te, (d) T = Cl, (e) T = Br, and (f) T = I.

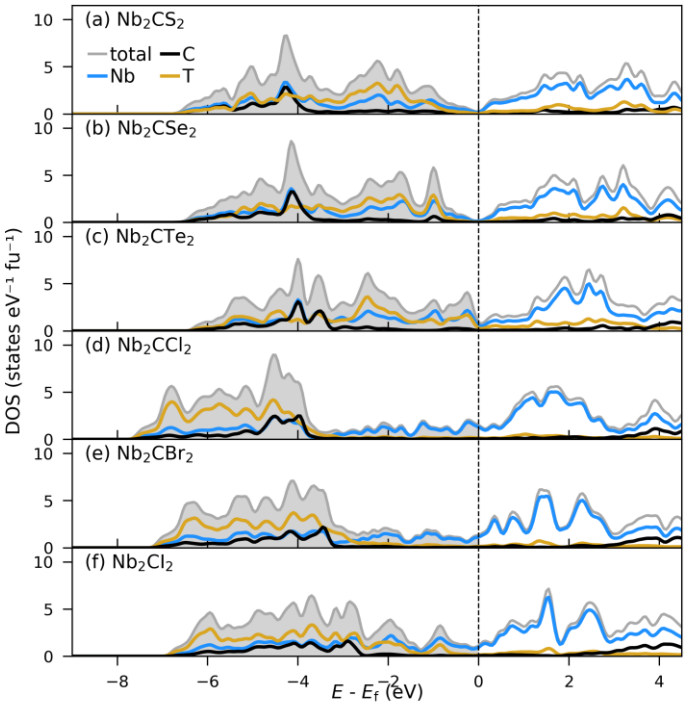

Figure S19. Electronic density of states for lowest energy structures of Nb_2CT_2 for (a) T = S, (b) T = Se, (c) T = Te, (d) T = Cl, (e) T = Br, and (f) T = I.

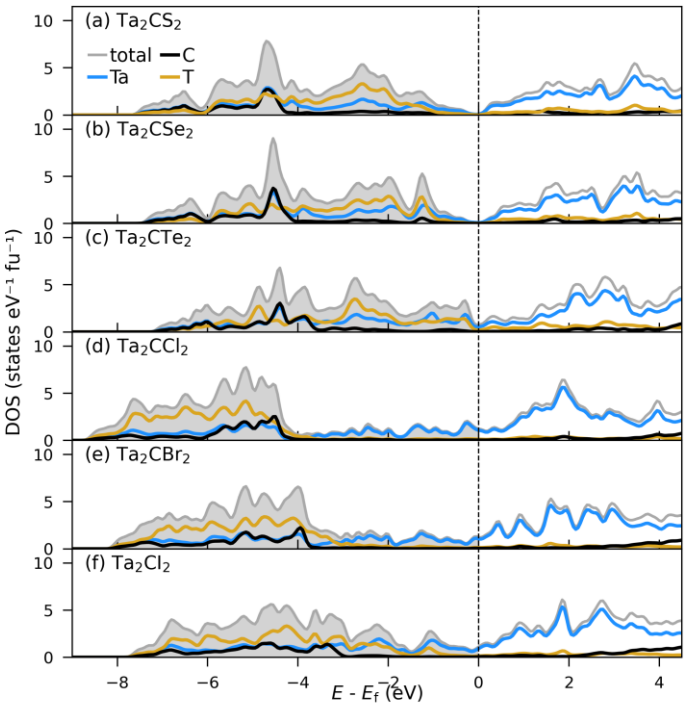

Figure S20. Electronic density of states for lowest energy structures of Ta_2CT_2 for (a) T = S, (b) T = Se, (c) T = Te, (d) T = Cl, (e) T = Br, and (f) T = I.

Ideal single-sheet M_2CT_2

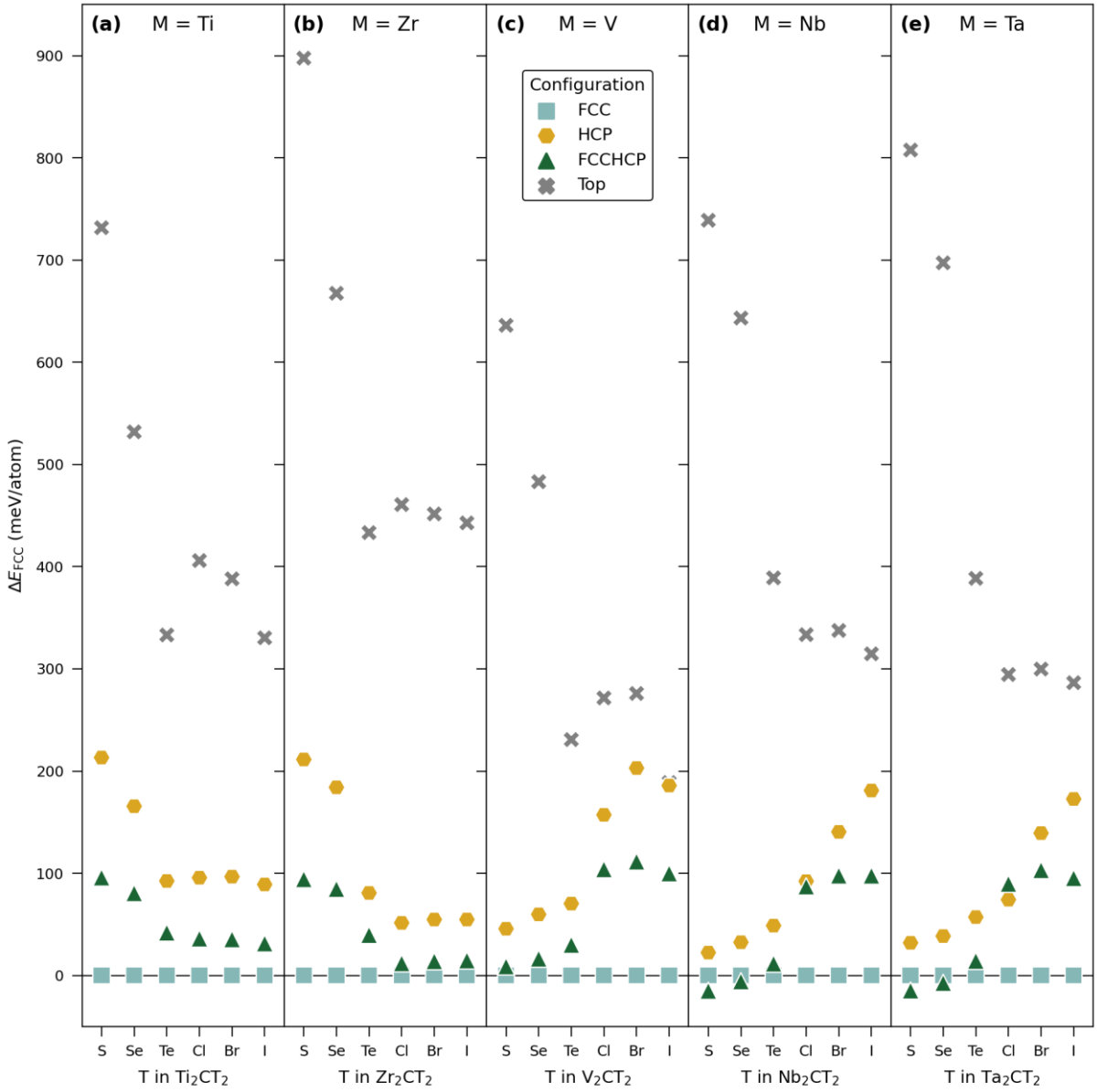

Figure S21. Single-sheet MXene with ideal termination coverage. Relative energies for various condfiurations compared to FCC using different termination T for (a) Ti_2CT_2, (b) Zr_2CT_2, (c) V_2CT_2, (d) Nb_2CT_2, and (e) Ta_2CT_2. The exchange–correlation interactions were treated by van der Waals density functional (DFT-D3) developed by Grimme et al. [35].

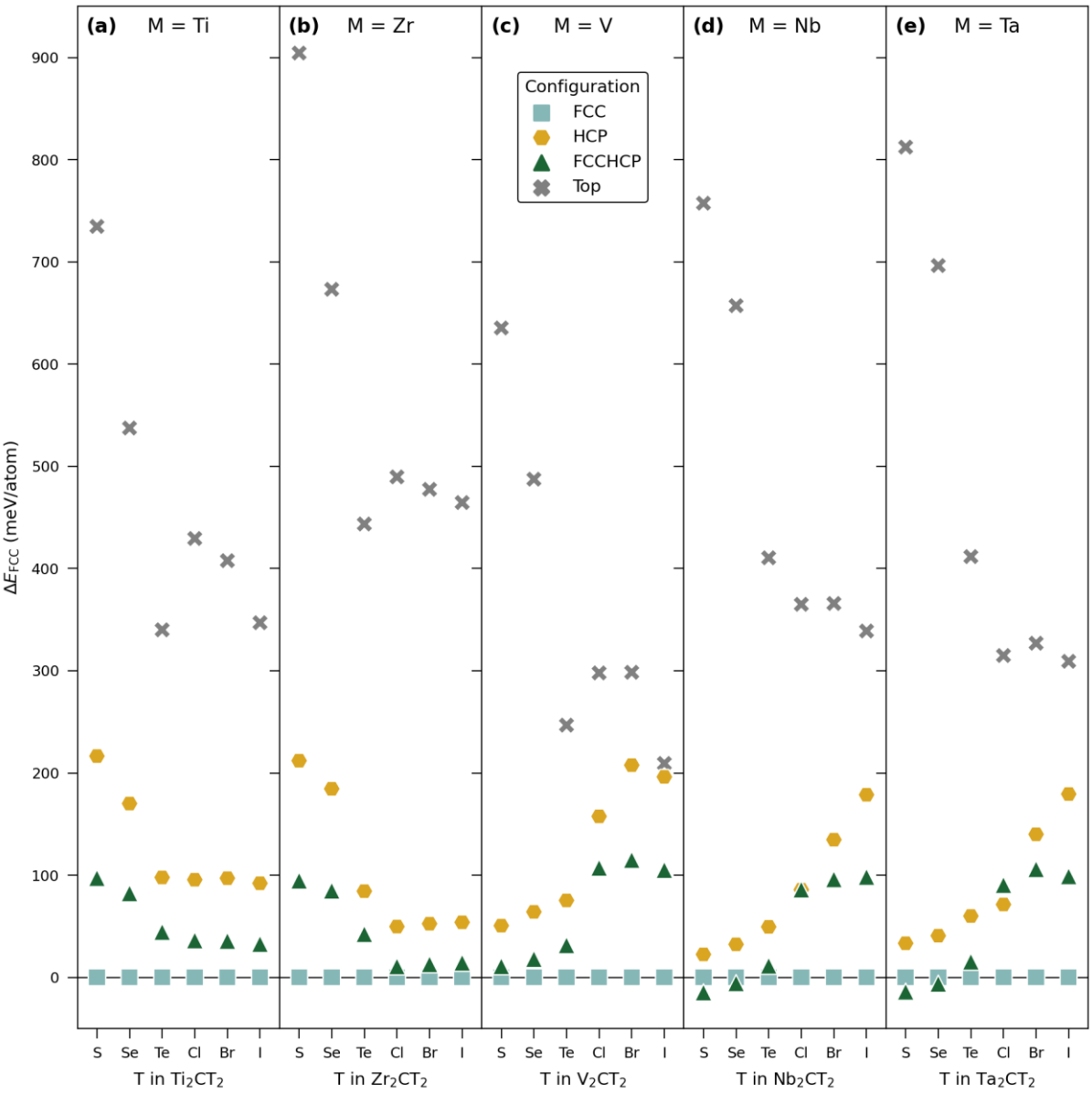

Figure S22. Single-sheet MXene with ideal termination coverage. Relative energies for various condfiurations compared to FCC using different termination T for (a) Ti_2CT_2, (b) Zr_2CT_2, (c) V_2CT_2, (d) Nb_2CT_2, and (e) Ta_2CT_2. The exchange–correlation interactions were treated by van der Waals density functional (rev-vdW-DF2) in the version developed by Hamada [36, 37].

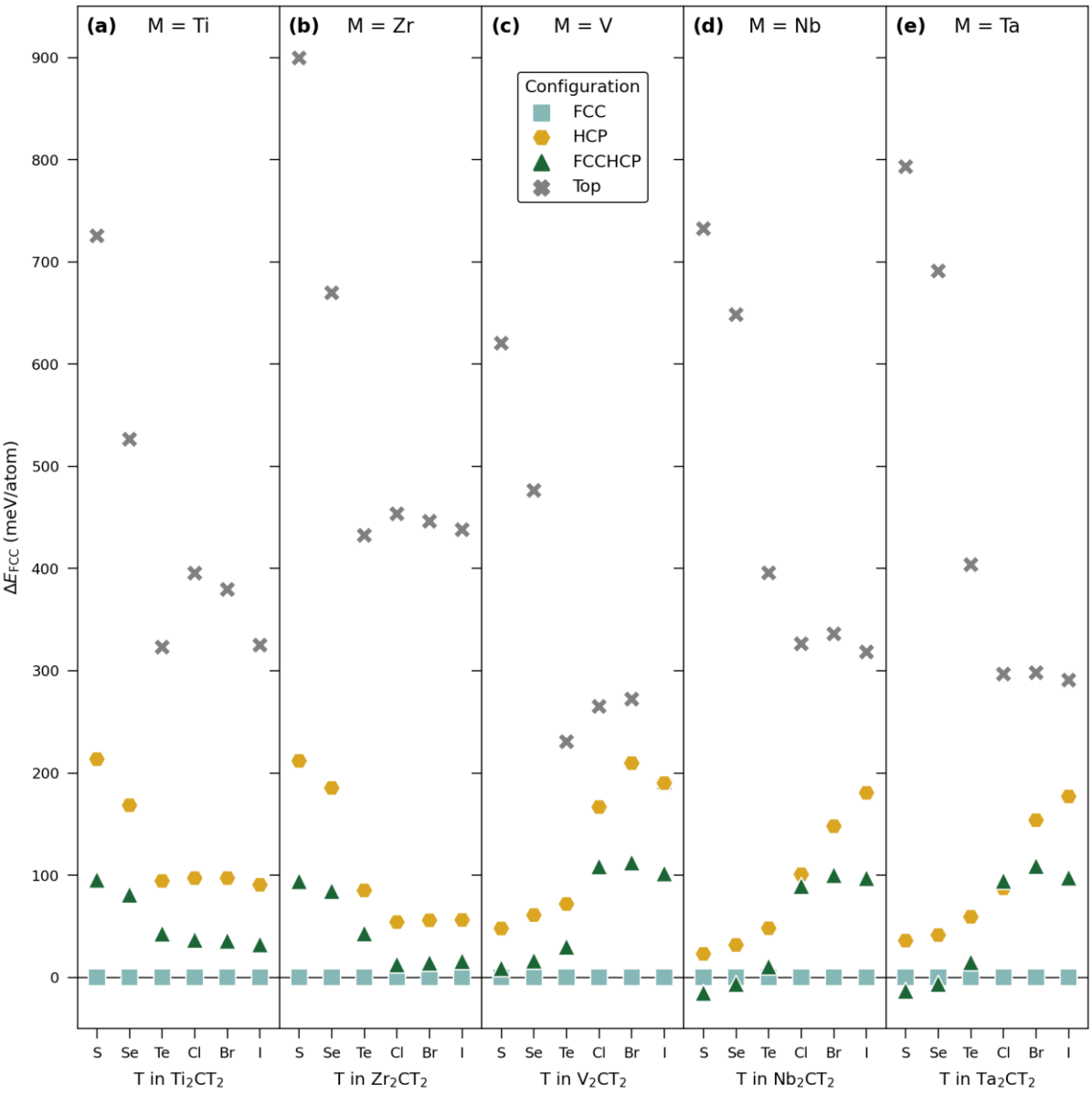

Figure S23. Single-sheet MXene with ideal termination coverage. Relative energies for various condfiurations compared to FCC using different termination T for (a) Ti_2CT_2, (b) Zr_2CT_2, (c) V_2CT_2, (d) Nb_2CT_2, and (e) Ta_2CT_2. No van der Waals interaction were considered.

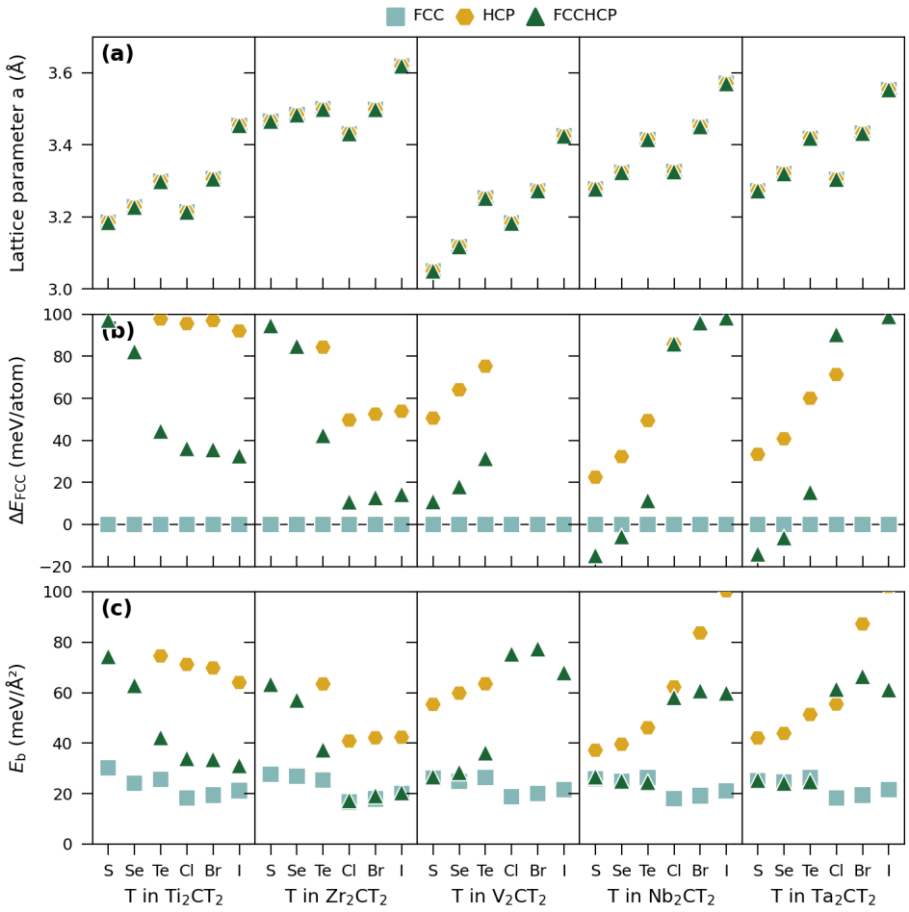

Figure S24. Single-sheet MXene with ideal termination coverage (a) In-plane lattice parameter *a* and (b) relative energies for various configurations compared to FCC terminated single-sheet M_2CT_2. (c) Binding energy E_b for different configurations of single-sheet M_2CT_2. The exchange–correlation interactions were treated by van der Waals density functional (rev-vdW-DF2) in the version developed by Hamada [36, 37].

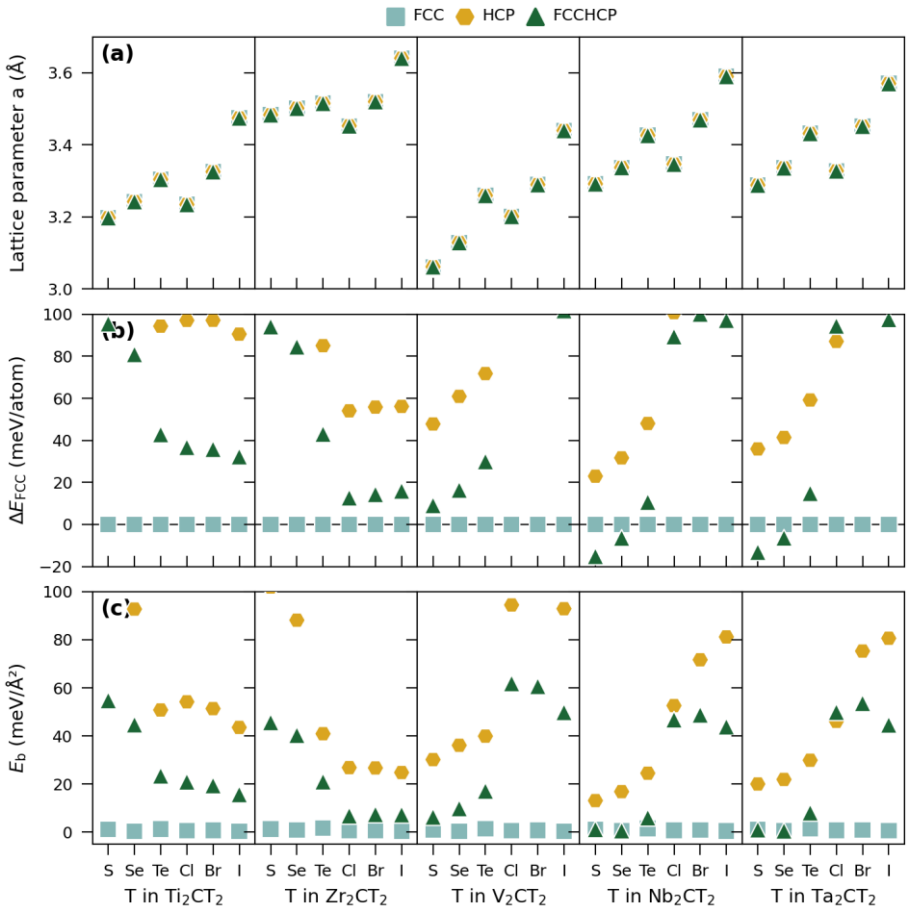

Figure S25. Single-sheet MXene with ideal termination coverage (a) In-plane lattice parameter *a* and (b) relative energies for various configurations compared to FCC terminated single-sheet M_2CT_2. (c) Binding energy E_b for different configurations of single-sheet M_2CT_2. No van der Waals interaction were considered.

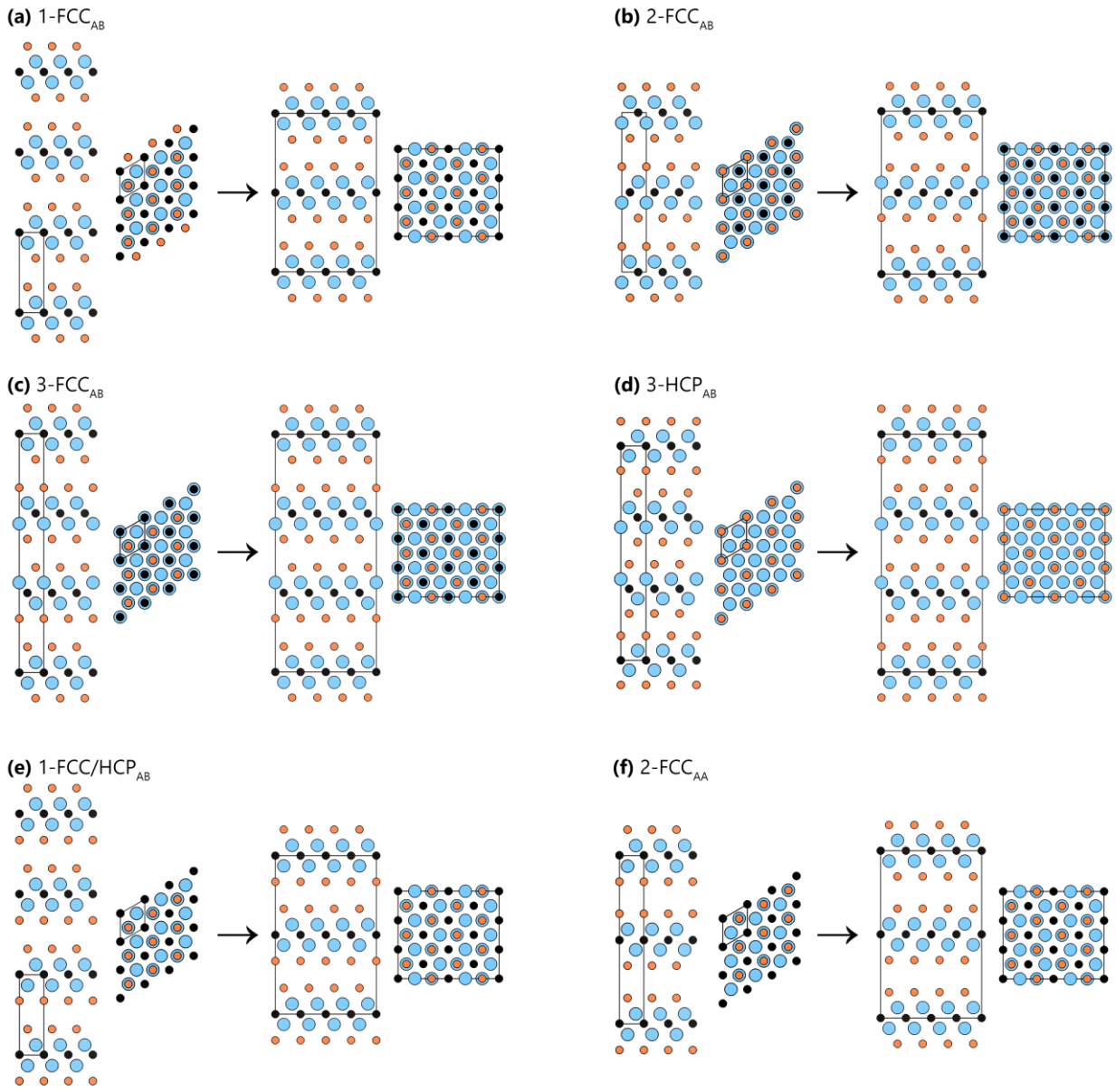

Figure S26. Schematic illustration of the relationship between the conventional unticell of M_2CT_2 and the supercells used for modeeling non-ideal termination coverage of M_2CT_x for (a) 1-FCC$_{AB}$, (b) 2-FCC$_{AB}$, (c) 3-FCC$_{AB}$, (d) 3-HCP$_{AB}$, (e) 1-FCC/HCP$_{AB}$, and (f) 2-FCC$_{AA}$. Metals in blue, carbon in black, and termination T in orange.

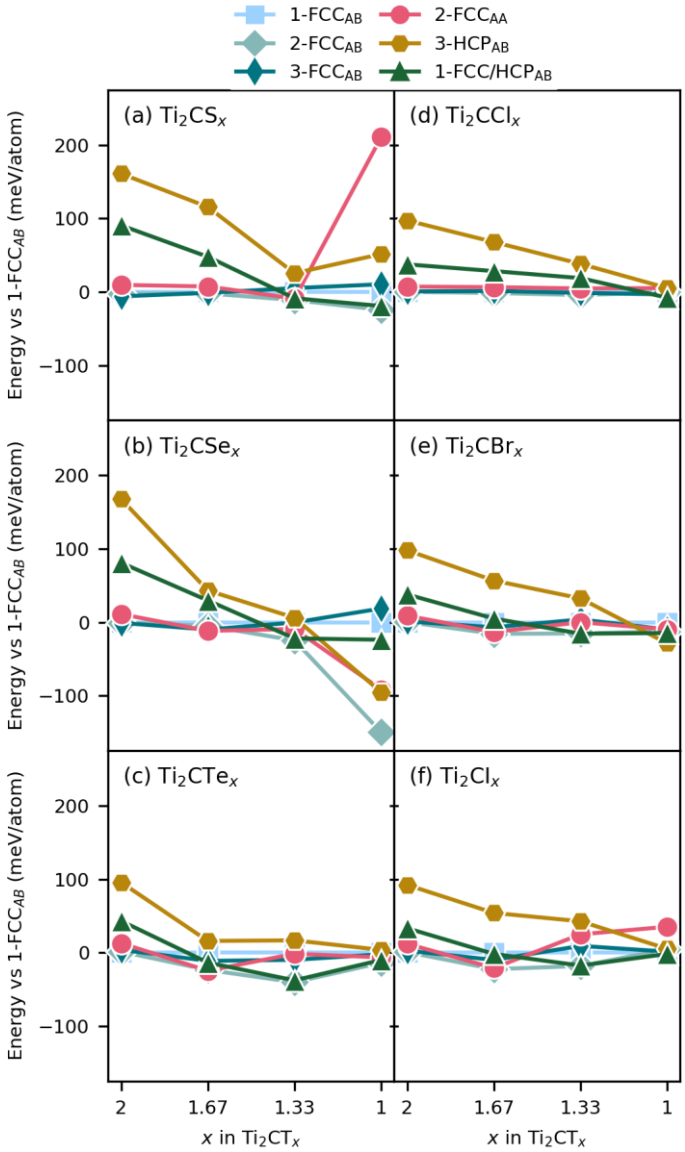

Figure S27. Multilayer MXene with non-ideal termination coverage. Energy of different stackings relative to 1-FCC$_{AB}$ as function of termination coverage x for Ti$_2$CT$_x$ where T is (a) S, (b) Se, (c) Te, (d) Cl, (e) Br, and (f).

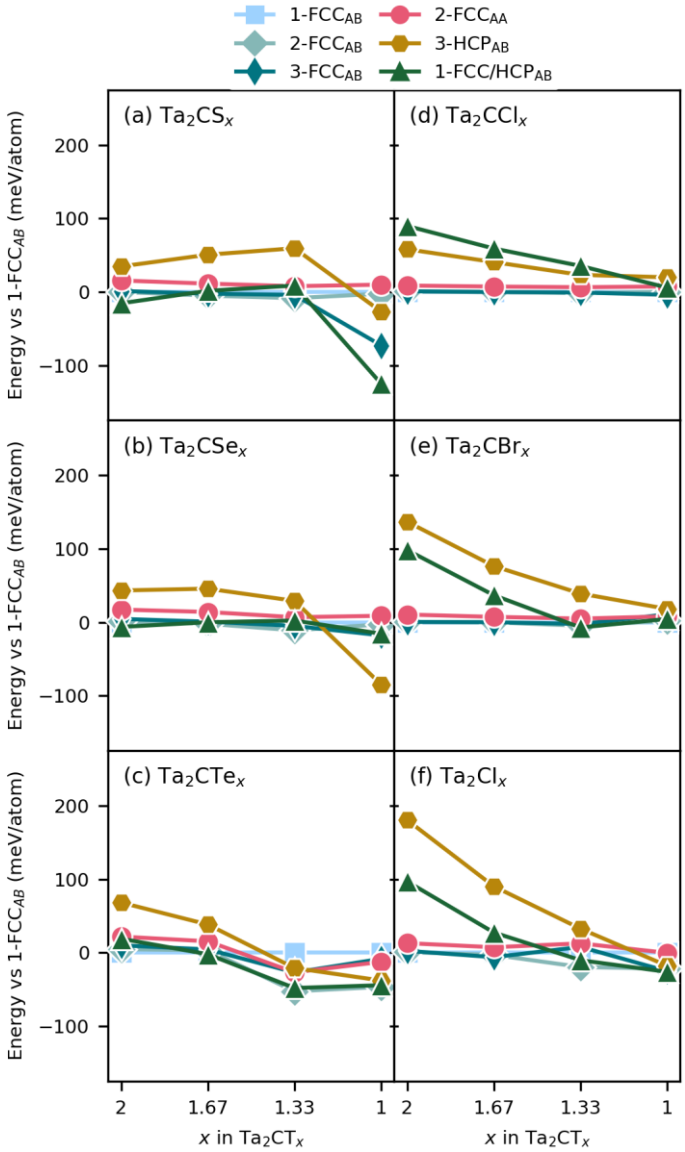

Figure S28. Multilayer MXene with non-ideal termination coverage. Energy of different stackings relative to 1-FCC$_{AB}$ as function of termination surface coverage x for Ta$_2$CT$_x$. where T is (a) S, (b) Se, (c) Te, (d) Cl, (e) Br, and (f).

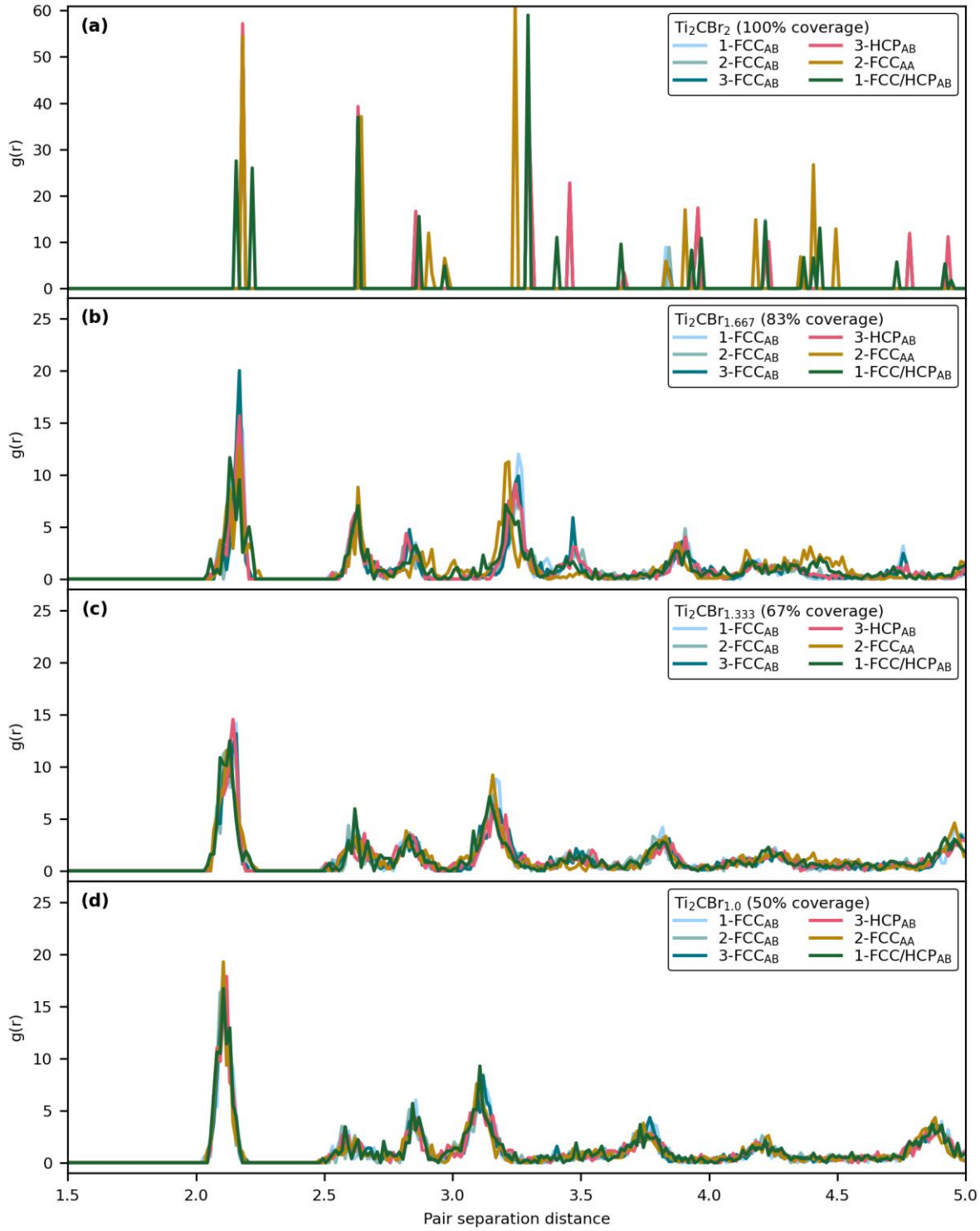

Figure S29. Radial distribtion function for Ti_2CBr_x for various stackings for (a) ideal termination coverage at x = 2 and at (c-d) non-ideal termination coverage at $x < 2$.

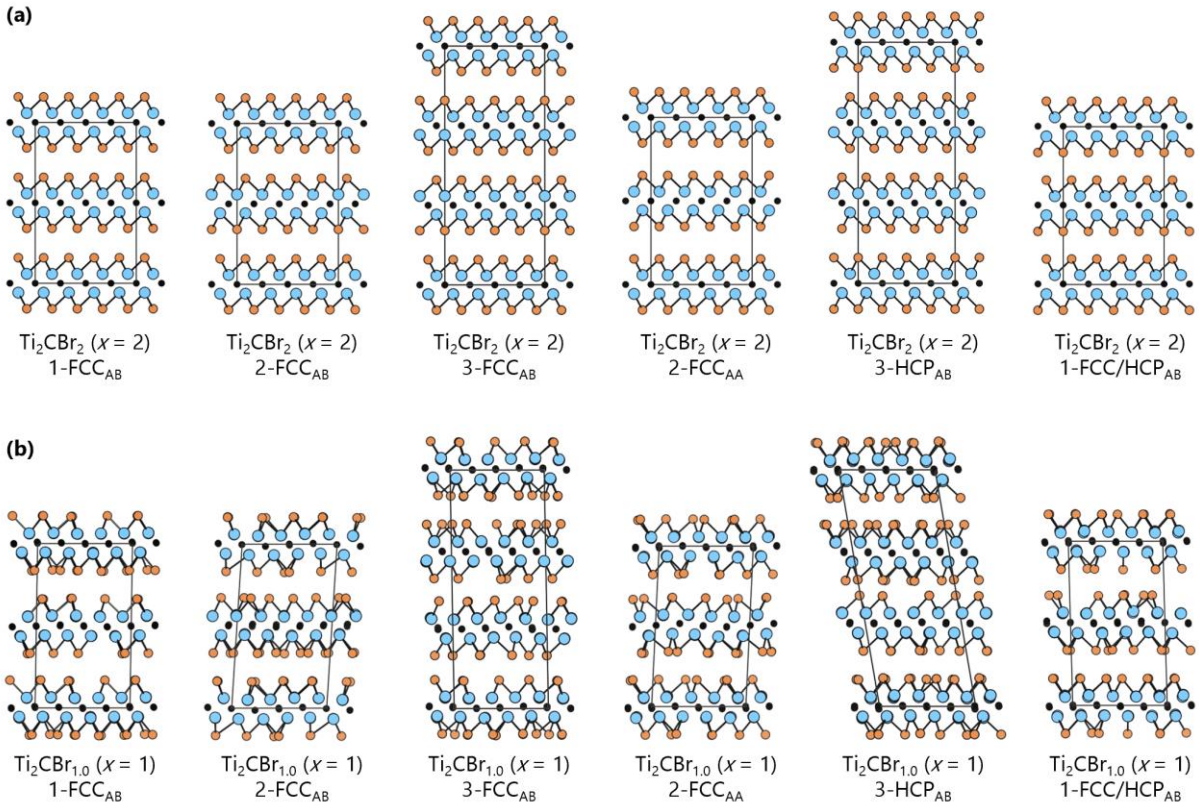

Figure S30: Schematic illustrations exemplfying the mixed termination sites for non-ideal termination coverage for multilayer MXenes. Here obsevered when comapring (a) 100% with (b) 50% termination coverage. Relaxed structures have been retrieved for Ti_2CBr_2 and $Ti_2CBr_{1.0}$ with different initial stacking configurations. Ti in blue, carbon in black, and Br in orange.

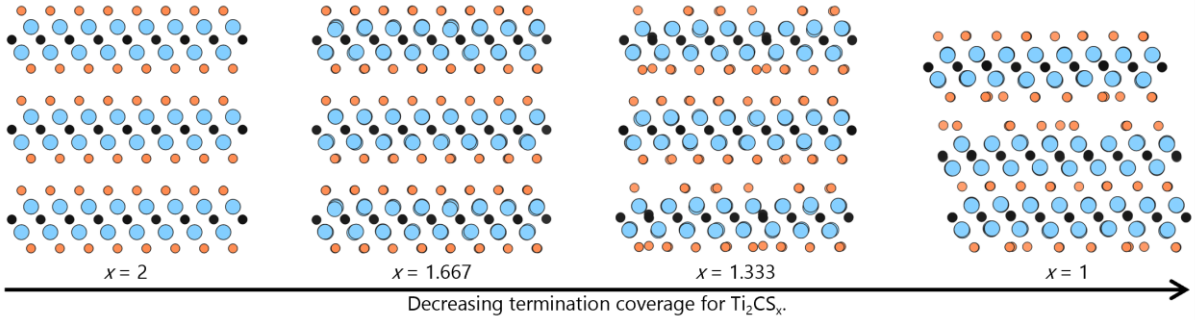

Figure S31. Schematic illustration exemplfying the structraul evolution when going from ideal termination coverage of $x = 2$ to an overall surface termination coverage of $x = 1$. Relaxed structures retrived for Ti_2CS_x with initial 1-FCC_{AB}. Note that for $x = 1$, one of the double T-layers have collpased into one. Ti in blue, carbon in black, and S in orange.

Single-sheet MXenes with non-ideal termination coverage

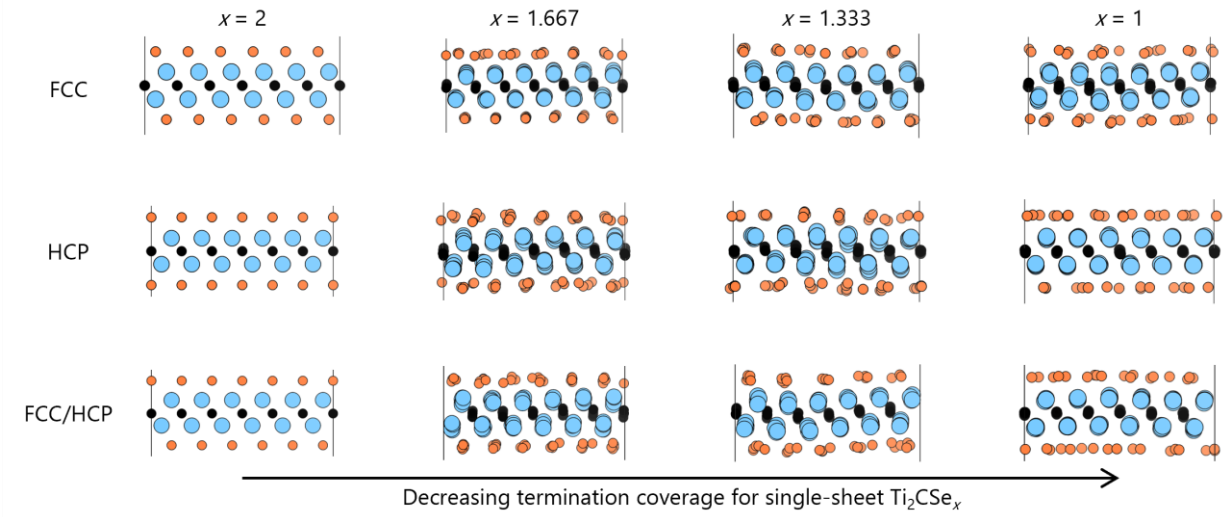

Figure S32. Schematic illustration from fully terminated singel-sheet MXene to 50% coverage for FCC, HCP, and FCC/HCP configurations demonstrating the evoloution into mixed termination sites at low enough coverage. Ti in blue, carbon in black, and Se in orange.